CHAPTER 26 ■ CARDIAC MASSES

JAY S. LEB AND SETH KLIGERMAN

INTRODUCTION

Cardiac masses are a relatively uncommon entity which can be classified as either a tumor or tumorlike condition. The prevalence of cardiac tumors is low, estimated at 0.002% to 0.03% on autopsy series. In fact, many of the cardiac lesions detected are usually tumorlike lesions, with thrombus representing most cases. Cardiac tumors can be further classified as primary or secondary, with secondary tumors due to metastatic disease being 20 to 40 times more common than primary cardiac tumors (Fig. 26.1). While the classification of theses lesions into benign or malignant entities is an important prognostic factor, any cardiac tumor or tumorlike condition can cause significant morbidity or mortality by causing embolic, arrhythmogenic, or obstructive manifestations. Advances in cardiac imaging, particularly cross-sectional imaging, have significantly expanded the role of imaging in the evaluation of these lesions.

IMAGING TECHNIQUES AND PROTOCOLS

Cardiac masses are often detected incidentally on routine echocardiography or computed tomography (CT) studies, performed for other reasons. With the increasing temporal resolution of conventional CT, there are an increasing number of incidental cardiac lesions detected on routine chest and abdominal imaging. Once discovered, localization of the lesion is the first important diagnostic step. Knowing the location of the lesion alone can aid in narrowing the differential diagnosis (Figs. 26.2 and 26.3). Many times, reported cardiac lesions either reflect normal structures or are related to extracardiac lesions from the adjacent structures, including the pericardium, mediastinum, or lungs. Visualization of the epicardium and/or pericardium can be helpful in distinguishing intra- versus extracardiac lesions. Localizing the epicenter of the lesion within the heart will aid in the diagnosis of cardiac masses. Detecting calcification, fat, or fibrous tissue within the lesion will help narrow the diagnosis. Imaging features can also aid in determining if the lesion has benign or malignant features (Table 26.1). Of course, one of the most crucial questions to answer is whether the lesion is a mass or a thrombus.

Echocardiography

Several imaging modalities are available to evaluate cardiac masses, each with different advantages and disadvantages. Transthoracic echocardiography remains the first-line imaging technique used to evaluate cardiac masses, as it is widely available, readily performed, and relatively inexpensive. It provides excellent real-time imaging to evaluate heart morphology, and ventricular and valvular function. However, the poor soft tissue contrast of echocardiography and its restricted acoustic windows limit its ability to completely characterize cardiac masses. Echocardiographic evaluation of the adjacent extracardiac structures is also limited and the extent of local involvement is not always assessed. In addition, large infiltrative extracardiac masses may be misinterpreted as primarily intracardiac in location due to the narrow field of view. While transesophageal echocardiography is superior in its available acoustic windows, it remains limited by its restricted fields of view and soft tissue contrast.

Cross-Sectional Imaging

With recent advances in techniques, cross-sectional imaging with cardiac CT and cardiac magnetic resonance imaging (CMR) is increasingly relied on for further evaluation of suspected cardiac lesions. ECG gating, the ability to time the imaging acquisition to the patient's electrocardiogram, limits motion artifact and can help provide functional analysis.

Cardiac CT. ECG-gated cardiac CT—with high spatial resolution, multiplanar image reconstruction capabilities, and fast acquisition times—allows for the accurate detection and localization of cardiac masses. Although the ability of CT to characterize tissue is not as good as MRI, CT is excellent in detecting the presence of fat, fluid, and calcification within lesions. Retrospective ECG gating, where the heart is imaged throughout the cardiac cycle, may be helpful to demonstrate movement of the mass during the cardiac cycle. Disadvantages of cardiac CT include decreased temporal resolution, exposure to ionizing radiation, and inferior soft tissue contrast as compared with MRI. The need for intravenous contrast limits CT availability in patients with renal failure or prior contrast allergy.

Intravenous, nonionic contrast is an important component in the CT evaluation of cardiac lesions. If the location

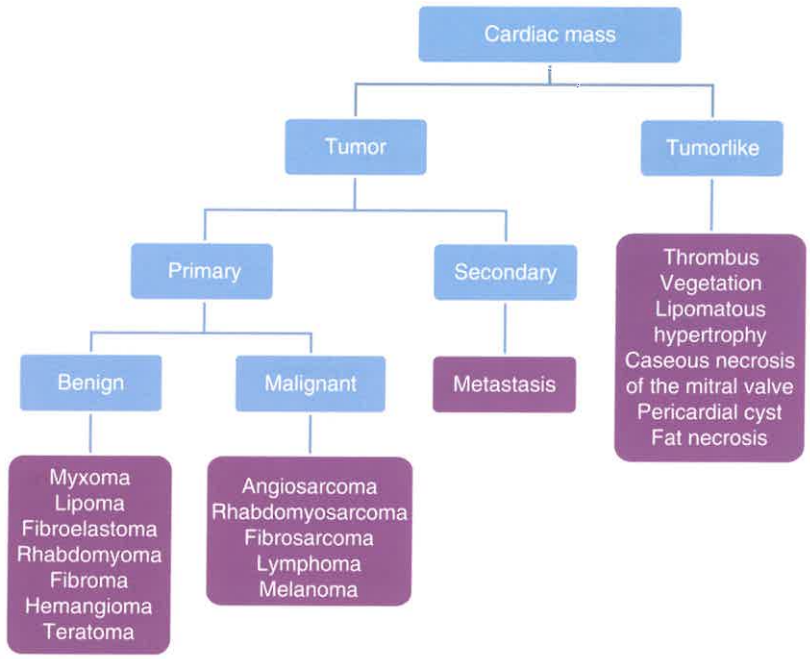

FIGURE 26.1. Overview of Cardiac Mass Subtypes.

of the lesion in question is known, the contrast timing can be tailored to opacify the region of interest by using either bolus tracking or timing-bolus techniques. Bolus tracking is performed by placing a region of interest in a specific area (depending on what needs to be opacified for the examination) and serial images are obtained, with subsequent triggering of the scan when the density within the region of interest exceeds a designated threshold value. Timing-bolus technique utilizes a preliminary scan using a small quantity of contrast (10 to 20 mL), and the transit time for the time for the contrast to peak (TTP) in the region of interest is calculated. Otherwise, a larger volume of contrast should be administered to ensure adequate opacification of all chambers. Delayed-phase imaging may be helpful in assessing tumor enhancement or to

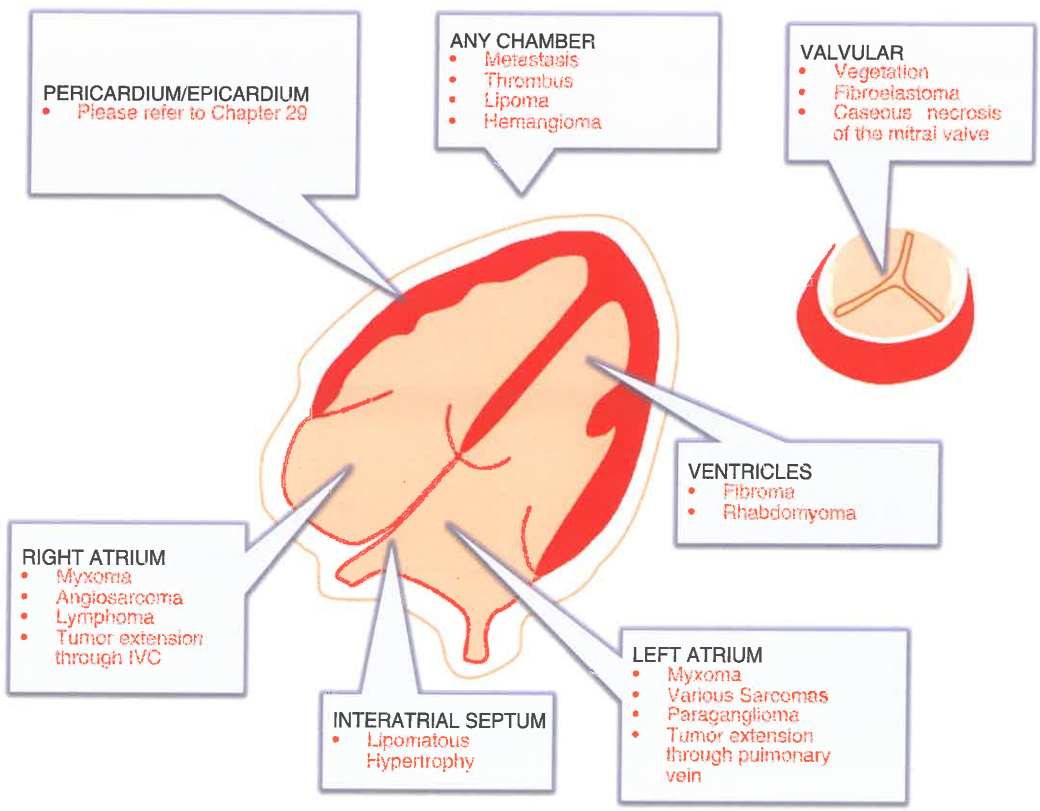

FIGURE 26.2. Schematic Depiction of the Typical Location of Common Cardiac Masses.

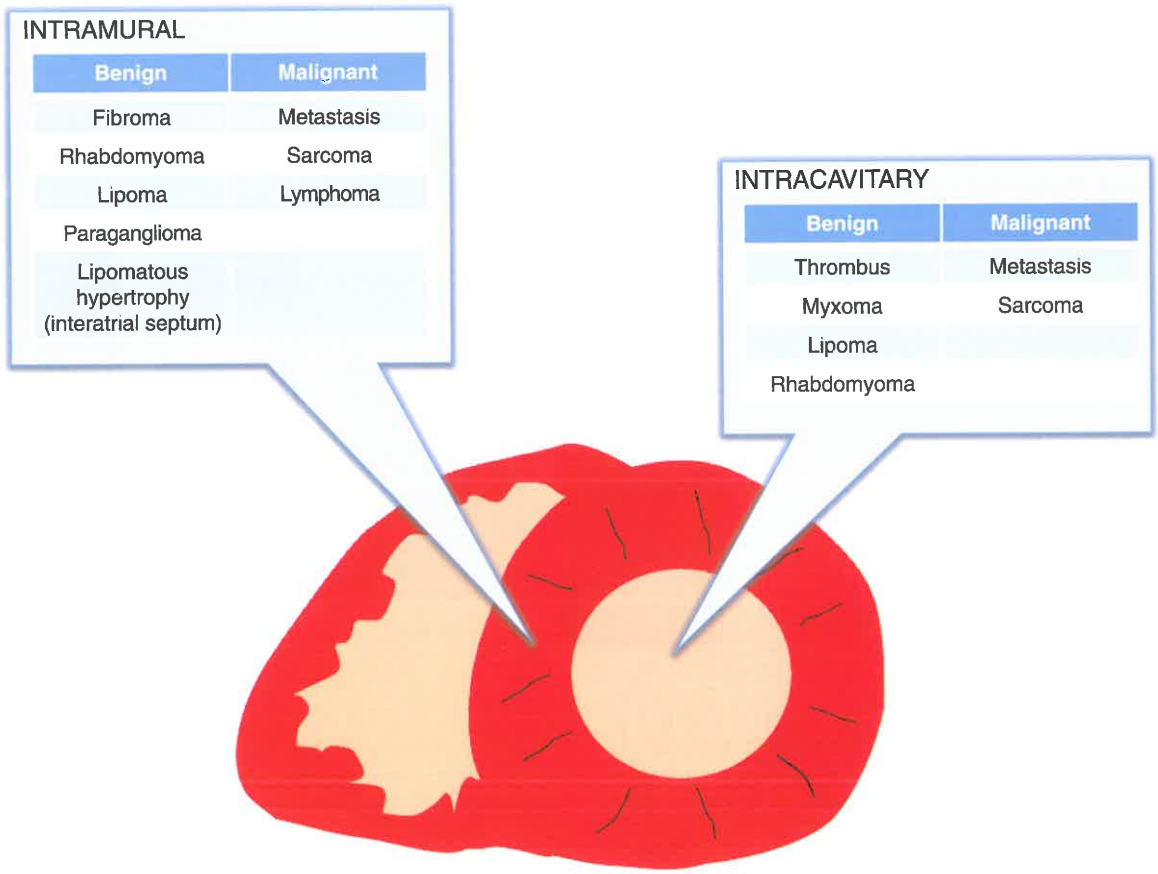

FIGURE 26.3. **Schematic Depiction of Common Cardiac Masses and Their Location With Relation to the Myocardium.**

improve opacification of the right atrium, IVC, or left atrial appendage.

Cardiac MRI. Cardiac MRI is currently the modality of choice in evaluating cardiac masses. It is noninvasive, offers multiplanar imaging, unrestricted fields of view, and provides excellent soft tissue contrast. Gradient echo cine imaging allows for excellent localization of the mass and simultaneously allows for functional analysis. T1- and T2-weighted imaging (T1W and T2W) provides valuable anatomic definition and tissue characterization. However, definitive differentiation between benign and malignant lesions based on these signal characteristics alone are difficult due to the wide overlap of many tumors, as most tumors demonstrate low to intermediate signal on T1W imaging and high signal on the T2W imaging. Fat-saturation techniques are routinely used to evaluate for the presence of fat. Postcontrast T1–based perfusion and late gadolinium enhancement (LGE) images are key sequences to evaluate for lesion vascularity and enhancement (Table 26.2).

The cardiac MR protocol is tailored to detect the lesion, evaluate its morphology, and define its tissue components. Scout images and nontargeted axial images of the chest are

TABLE 26.1

BENIGN VERSUS MALIGNANT IMAGING FEATURES

FEATURES	BENIGN	MALIGNANT
Size	▪ Small, <5 cm	▪ Large, >5 cm
Number of lesions	▪ Single	▪ Multiple
Location	▪ Left sided	▪ Right sided
Margins	▪ Smooth ▪ Well-defined borders ▪ No extension through tissue planes	▪ Irregular ▪ Ill-defined borders ▪ Direct invasion through tissue planes
Pericardium	▪ No involvement	▪ Hemorrhagic pericardial effusion ▪ Pericardial invasion or multiple nodular masses
Tissue characteristics	▪ Homogeneous ▪ Absent to minimal early enhancement. ▪ Variable delayed enhancement	▪ Heterogeneous due to hemorrhage and necrosis ▪ Prominent early enhancement. ▪ Variable delayed enhancement

TABLE 26.2

SUMMARY AND EXPLANATION OF THE CARDIAC MR SEQUENCES UTILIZED IN THE DETECTION AND EVALUATION OF CARDIAC MASSES

SEQUENCES	DESCRIPTION	UTILITY
3D scout images and transaxial images	▪ Either SSFP or FSE ▪ Large field of view ▪ Covers the entire thorax	▪ Overview of anatomy ▪ Visualization of large lesions involving the mediastinum/lungs
Cine SSFP	▪ Performed in the standard two-chamber, four-chamber, and stacked short-axis views ▪ Can also be performed in planes to optimally visualize the lesion	▪ Confirmation/localization of the lesion ▪ Assesses lesion size, mobility, effect on the myocardial function, and valvular structures
T1W +/– fat saturation	▪ T1W black blood double IR FSE images; triple IR used to null fat	▪ T1 tissue characterization ▪ Assesses for fat components, hemorrhage, or necrosis
T2W +/– fat saturation	▪ T2W black blood double IR FSE images; triple IR used to null fat	▪ T2 tissue characterization ▪ Assesses for edema or necrosis
Myocardial tagging (optional)	▪ Different tagging sequence techniques can be utilized	▪ Evaluates for the presence of infiltration into the myocardium or pericardium ▪ Detection of a noncontractile intramyocardial mass
Perfusion imaging	▪ During the administration of gadolinium (0.1–0.2 mmol/kg) ▪ Dynamic FLASH imaging	▪ Assesses lesion vascularity and distinguishes from myocardium or thrombus
Early postcontrast T1W	▪ 3D volumetric breath-hold T1 fat-saturated or T1W double IR FSE images	▪ Assesses lesion enhancement and distinguishes from myocardium or thrombus
Late gadolinium enhancement	▪ 10 minutes after contrast injection ▪ Segmented double inversion recovery FSE sequence ▪ Inversion time (typically 200–300 ms) set to achieve appropriate nulling of the normal myocardium, determined via a TI scout or Look–Locker sequence	▪ Assesses lesion enhancement and distinguishes from myocardium or thrombus ▪ Can also perform imaging at an inversion time of 600 ms to aid in distinguishing thrombus versus mass

first utilized to help locate the lesion and plan subsequent targeted imaging. Steady-state free precession (SSFP) cine images are then performed and prescribed based on the location of the mass. In general, the entire mass should be evaluated in at least one plane to ensure accurate characterization. After the mass is localized, T1W and T2W sequences should be obtained through the lesion prior to contrast administration to characterize the tissue types. In lesions localized near or within the pericardium, myocardial tissue tagging—a dynamic tagged sequence—can aid in the detection of myocardial infiltration or adhesions. In addition, tagging sequences can help detect the presence of a noncontractile intramyocardial mass, such as a rhabdomyoma, or differentiate a true mass versus asymmetric focal hypertrophic cardiomyopathy.

After localization and basic tissue characterization, postcontrast imaging following the intravenous administration of gadolinium-based contrast is a key component to the MR evaluation. The tumor should be imaged during first-pass perfusion to allow for detection of early arterial enhancement. Afterward, T1-postcontrast imaging should be performed in the same plane as the T1W precontrast images to allow for accurate comparison. LGE images are performed 10 to 15 minutes after the administration of contrast, which is useful to detect late gadolinium enhancement of the mass or surrounding myocardial enhancement due to the mass. The LGE characteristics may help differentiate thrombus or other benign lesions from the malignant ones which typically demonstrate increasingly greater enhancement. Utilizing longer inversion recovery times (such as 600 ms) can distinguish a thrombus from a tumor.

While an excellent tool for cardiac mass evaluation, MRI does have its limitations. First off, MRI examinations require a patient to lie supine in a relatively enclosed tube for a prolonged period, often greater than 1 hour. Sedation may be necessary for patients with severe claustrophobia or those who cannot follow instructions. This can prolong imaging time due to the need to perform multiaverage sequences. In addition, small masses may not be detected on MRI due to its relatively decreased spatial resolution compared to other modalities such as CT (Table 26.3).

BENIGN CARDIAC TUMORS

Myxoma. Myxomas are benign lesions of endocardial origin. They are the most common primary cardiac tumor and represent 50% of all benign cardiac masses and 25% of all primary cardiac tumors. They usually occur in the fourth to seventh decades of life and approximately 60% of affected patients are female. Myxomas arise from undifferentiated and totipotent mesenchymal stem cell and have a gelatinous composition described as an acid mucopolysaccharide–rich stroma. Greater than 90% of cases are sporadic and usually solitary. However, cardiac myxomas can be seen in patients with the Carney complex, which is an autosomal dominant disorder characterized by an increased risk of tumors including cardiac and

TABLE 26.3

SUMMARY OF CARDIAC MASS IMAGING FEATURES ON CT AND MRI

CARDIAC LESION	LOCATION	CT FEATURES	T1W	T2W	PERFUSION/T1W+	LGE	OTHER
Myxoma	Left atrium, interatrial septum attached to the fossa ovalis	Hypodense lesion	Isointense	Hyperintense areas	Mild	Heterogeneous	Lobular, at times on a stalk
Lipoma	Endocardial, intramyocardial, or epicardial in or around any chamber	Homogenous lesion with fat density	Hyperintense	Hyperintense	Absent	Absent	Suppresses on fat suppression images
Papillary fibroelastoma	Valve leaflets, most commonly the aortic	Small mobile homogenous lesion	Hypo/ Isointense	Iso/hyperintense	Absent	Variable but usually moderate	Unlike vegetation, will not typically cause valvular destruction
Rhabdomyoma	Ventricles, intramyocardial or intracavitary	Smooth nodules in the myocardium	Isointense	Iso/hyperintense	Absent/mild	Absent/minimal	Frequently multifocal
Fibroma	Ventricles, intramyocardial	Homogenous low attenuation mass	Isointense	Hypointense	Absent	Intense	No enhancement on perfusion imaging due to avascularity
Hemangioma	Any chamber, intracavitary	Heterogeneous lesion, may have calcification	Iso/hyperintense	Hyperintense	Intense	Intense	Hypervascular on perfusion
Paraganglioma	Left atrium, the atrial roof or posterior wall	Well defined lesion with intense enhancement	Hypo/isointense	Hyperintense	Intense	Intense	Light bulb bright on T2W
Metastasis	Endocardial, intramyocardial, or epicardial in or around any chamber	Infiltrative lesion	Variable, commonly hypointense	Hyperintense	Variable (mild to intense)	Heterogeneous	Melanoma will be high on T1W and low on T2W
Angiosarcoma	Right atrium/ventricle	Hemorrhagic lesion	Heterogeneous	hyperintense	Intense	Heterogenous	May have pericardial involvement with a hemorrhagic effusion
Other sarcomas	Left atrium	Usually hypodense	Hypo/isointense	Hyperintense	Moderate/intense	Heterogeneous/ homogenous	Can extend into the pulmonary veins
Lymphoma	Anywhere but classically near right AV groove	Infiltrating lesion, low/ isoattenuating to the myocardium	Hypo/isointense	Iso/hyperintense	Absent/mild	Variable, at times none	Infiltrative tumor which grows along framework of heart
Thrombus	Any chamber	Homogenous lesion	Hypointense	Hypointense	Absent	Absent	Nulls at longer inversion time, around 600 msec
Lipomatous hypertrophy of the interatrial septum	Interatrial septum, always spares the fossa ovalis	Homogenous lesion with fat density	Hyperintense	Hyperintense	Absent	Absent	Suppresses on fat suppression images, barbell in shape

cutaneous myxomas. Other Carney complex associations include hyperpigmented skin lesions, endocrinopathy, and extracardiac neoplasms such as breast fibroadenomas, melanotic schwannomas, or pituitary adenomas. In cases where myxomas are multifocal, extra-atrial, or recurrent, association with the Carney complex should be suspected.

There is a varied clinical presentation in patients with a cardiac myxoma, depending on the lesion location, size, and its effect on cardiac function. The triad of intracardiac obstruction, embolization of tumor, and constitutional symptoms is classically described. Since the majority of tumors occur in the left atrium, symptoms are commonly related to mitral valve obstruction and include dyspnea and orthopnea from pulmonary edema (Fig. 26.4b). Right atrial tumors can present with findings of tricuspid valve obstruction, including peripheral edema and syncope.

As demonstrated on imaging, myxomas are commonly intracavitary with 75% to 80% of myxomas found in the left atrium, with the majority arising from the interatrial septum near the fossa ovalis. A minority of cases may arise from the chamber walls or valve surfaces. Larger tumors may obstruct or prolapse through the mitral valve. Ten to twenty percent of tumors occur in the right atrium. Myxomas originating in the ventricular chamber or atrioventricular valves are rare. Most cardiac myxomas are well-defined lesions which are ovoid or round in shape (Fig. 26.4A). They may be pedunculated on a discrete stalk or have a broad stalk or base of attachment with the pedunculated lesions having an increased chance of prolapsing and obstructing the adjacent atrioventricular valve. While the majority of myxomas are smooth or lobulated, there is a subset of villous or papillary myxomas which has multiple fragile, villous extensions, increasing the risk for embolization. Embolization is of much greater concern for left atrial masses due to the downstream systemic circulation (Fig. 26.4B).

Aside from lesion detection and localization, imaging will aid in lesion characterization. On echocardiography, myxomas may be homogeneous or heterogeneous, with hyperechoic areas representing focal calcification and hypoechoic regions relating to cystic, necrotic, or hemorrhagic components. In general, echocardiography is an excellent tool to visualize the myxoma's effect on surrounding structures, including valvular obstruction. On CT, myxomas are usually hypodense masses attached to the interatrial septum in the region of the fossa ovalis and may enhance heterogeneously with contrast administration. CT is an excellent tool for detection of calcification, which is visible in approximately 10% of cases. On MRI, myxomas classically demonstrate isointense signal on T1W images and hyperintense signal on T2W images. However, because myxomas have varying components within them, including hemorrhagic, myxomatous, cystic, fibrous, and/or necrotic tissue, many are heterogeneous in signal. The lesion is usually hyperintense to myocardium on bright-blood SSFP sequences and will enhance following the administration of gadolinium-based contrast agents (Fig. 26.4A,B). For most cases of cardiac myxomas, the key imaging feature in the diagnosis remains its location and relationship with the interatrial septum. When in this characteristic location, there is little else in the differential diagnosis. When in an atypical location, the differential diagnosis can include a variety of tumors including benign tumors such as fibroelastomas, hemangiomas, and malignancies such as metastases.

Lipoma. Intracardiac lipomas are benign lesions which constitute approximately 10% of all primary cardiac tumors. Lipomas consist of encapsulated mature adipose cells which are commonly well defined, round or oval in shape, and broad-based. The majority of cases arise from the epicardial surface and extend outward into the pericardial space. However, lipomas

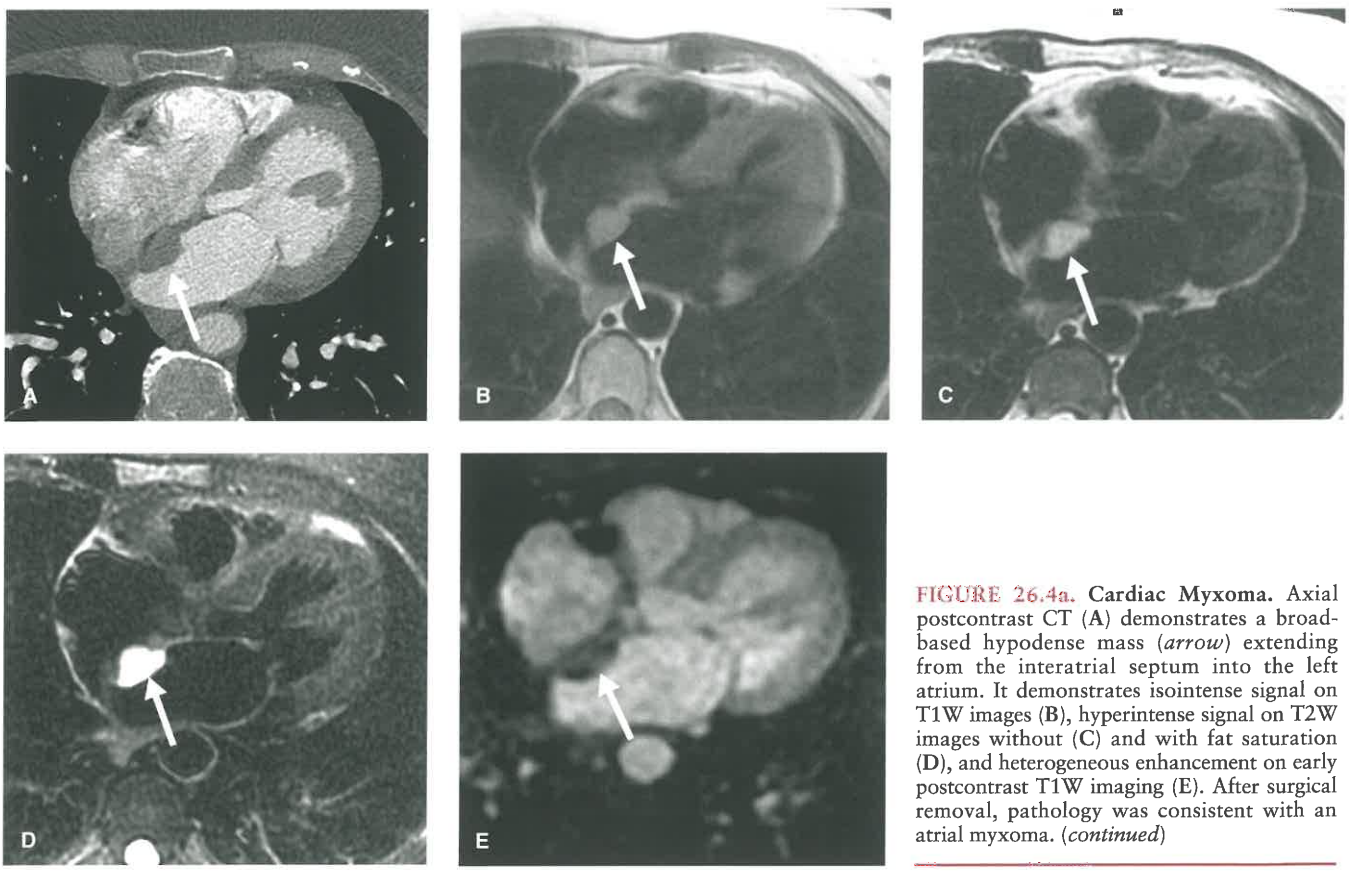

FIGURE 26.4a. **Cardiac Myxoma.** Axial postcontrast CT (**A**) demonstrates a broad-based hypodense mass (*arrow*) extending from the interatrial septum into the left atrium. It demonstrates isointense signal on T1W images (**B**), hyperintense signal on T2W images without (**C**) and with fat saturation (**D**), and heterogeneous enhancement on early postcontrast T1W imaging (**E**). After surgical removal, pathology was consistent with an atrial myxoma. (*continued*)

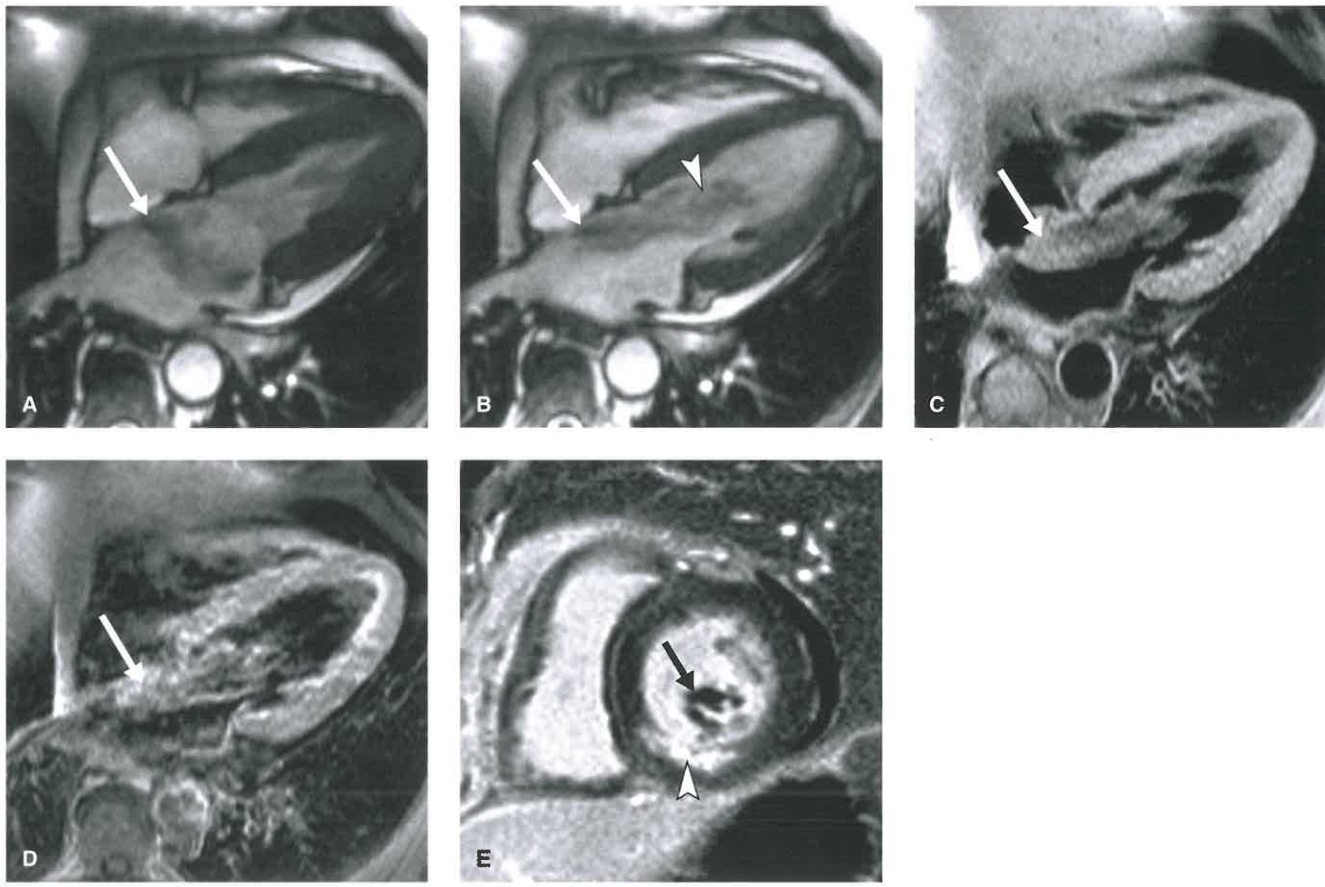

FIGURE 26.4b. (*Continued*) Villous cardiac myxoma with embolization into the right coronary artery in a 40-year-old woman. 4-chamber SSFP images obtained during systole (**A**) and diastole (**B**) shows a large left atrial mass attached to the region of the fossa ovalis (*white arrows*). The edges of the mass are ill-defined. During diastole, the mass prolapses through the mitral valve into the left ventricle (*white arrowhead,* **B**). On T1 weighted precontrast image (**C**), the mass is predominantly isointense to hypointense in signal compared to the myocardium. The mass shows heterogenous enhancement on T1W post-contrast imaging (**D**) which ranged from hypointense to hyperintense (*white arrow,* **D**) to myocardium. Delayed enhancement image (**E**) shows subendocardial infarct in the inferior wall due to RCA territory infarct (*white arrowhead*). Portions of the tumor can be seen in the left ventricle (*black arrow*). Myxoma tumor thrombus was removed from the RCA during cardiac catheterization and confirmed pathologically.

can also arise from the endocardium and pericardium. Most cases are asymptomatic and often discovered incidentally; however, larger lesions can cause obstruction to flow or impinge on ventricular wall motion when located in the pericardial space.

On CT, lipomas are homogeneous, well-defined lesions demonstrating density within the fatty range measuring less than –50 HU. On MRI, lipomas will follow fat signal on all sequences, decrease in signal with fat-suppression techniques, and will not demonstrate enhancement. The presence of a chemical shift/"India ink" artifact at the interface between the lipoma and the surrounding tissue on SSFP sequences is another characteristic finding (Fig. 26.5). While both cardiac lipomas and lipomatous hypertrophy of the interatrial septum will demonstrate identical signal characteristics, the location of the lesion within the interatrial septum with sparing of the fossa ovalis will allow differentiation of lipomatous hypertrophy from a true lipoma.

Papillary Fibroelastoma. Papillary fibroelastomas are benign endocardial–based lesions which constitute approximately 10% of all primary cardiac tumors. Fibroelastomas contain avascular dense connective tissue covered in a single layer of endothelium. They are generally small in size, measuring less than 1 to 1.5 cm on average. Pathologically, they have multiple papillary frond-like projections which are attached by a stalk-like projection to the valvular endocardium. Their appearance on gross pathologic examination has been compared to a sea anemone. Ninety percent of fibroelastomas occur on cardiac valves and they account for 75% of all valvular neoplasms. However, as they can occur on any endocardial surface, they should remain in the differential diagnosis when an endocardial-based mass is present. Most occur on the aortic and mitral valves and are usually located on the aortic side of the aortic valve and the atrial side of the atrioventricular valves, away from the free edge of the leaflet. No known familial cases of papillary fibroelastomas have been reported and they are usually solitary. Most cases of papillary fibroelastoma are asymptomatic and discovered incidentally; however, due to their friable nature and propensity for thrombus formation on their surface, there is an association with transient ischemic attacks and strokes.

Echocardiography is usually the best modality to detect and evaluate papillary fibroelastomas. The excellent temporal resolution of ultrasound allows for detection of these small, highly mobile lesions which are attached to the valve leaflets. Fibroelastomas will appear as homogeneous soft tissue attenuation lesions on ECG-gated CT, which can be used for presurgical planning (Fig. 26.6). On MRI, the lesions will demonstrate intermediate signal on T1W images and hyperintense signal on T2W images. Cine SSFP MR sequences may demonstrate turbulent flow surrounding the low signal mass. While there may be mild enhancement on T1W postcontrast imaging, fibroelastomas often show intense enhancement on delayed enhancement sequences obtained 10 minutes after the administration of intravenous contrast due to the presence of

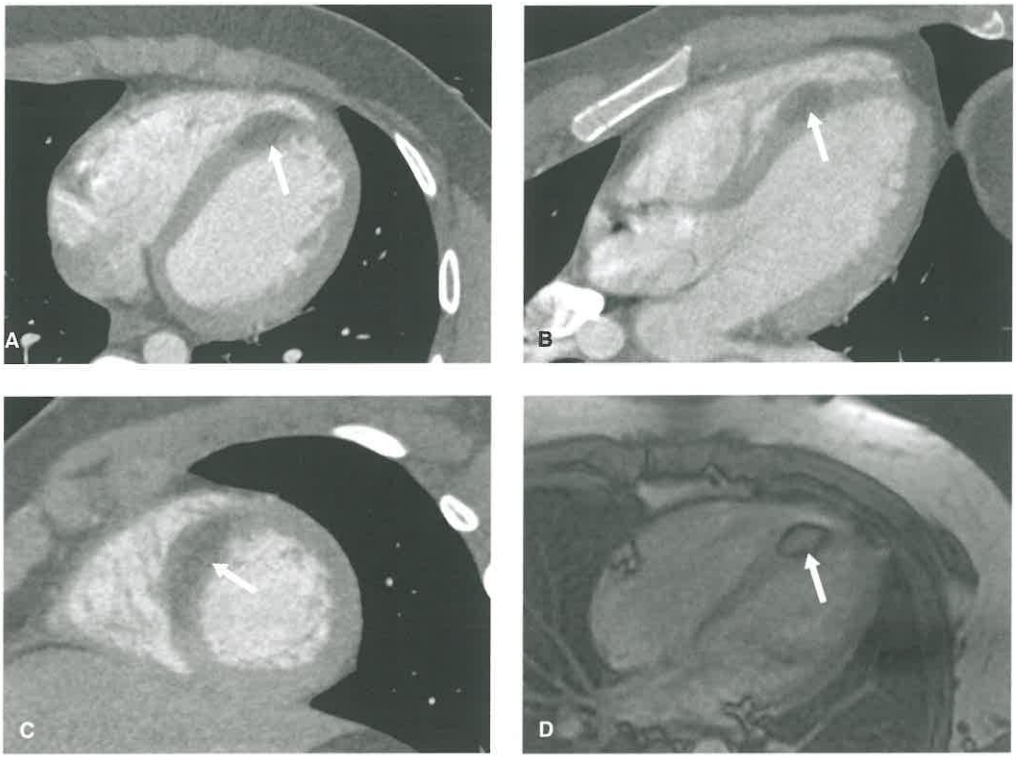

FIGURE 26.5. **Cardiac Lipoma.** Axial CT image (A) with multiplanar reconstructions in the three-chamber (B) and short-axis (C) views demonstrates a hypodense intramural mass (*arrow*) in the apical interventricular septal segment. Axial SSFP MR image (D) demonstrates peripheral "India ink" artifact (*arrow*) indicating the presence of a fat-containing lesion. These findings are most consistent with an intramyocardial lipoma.

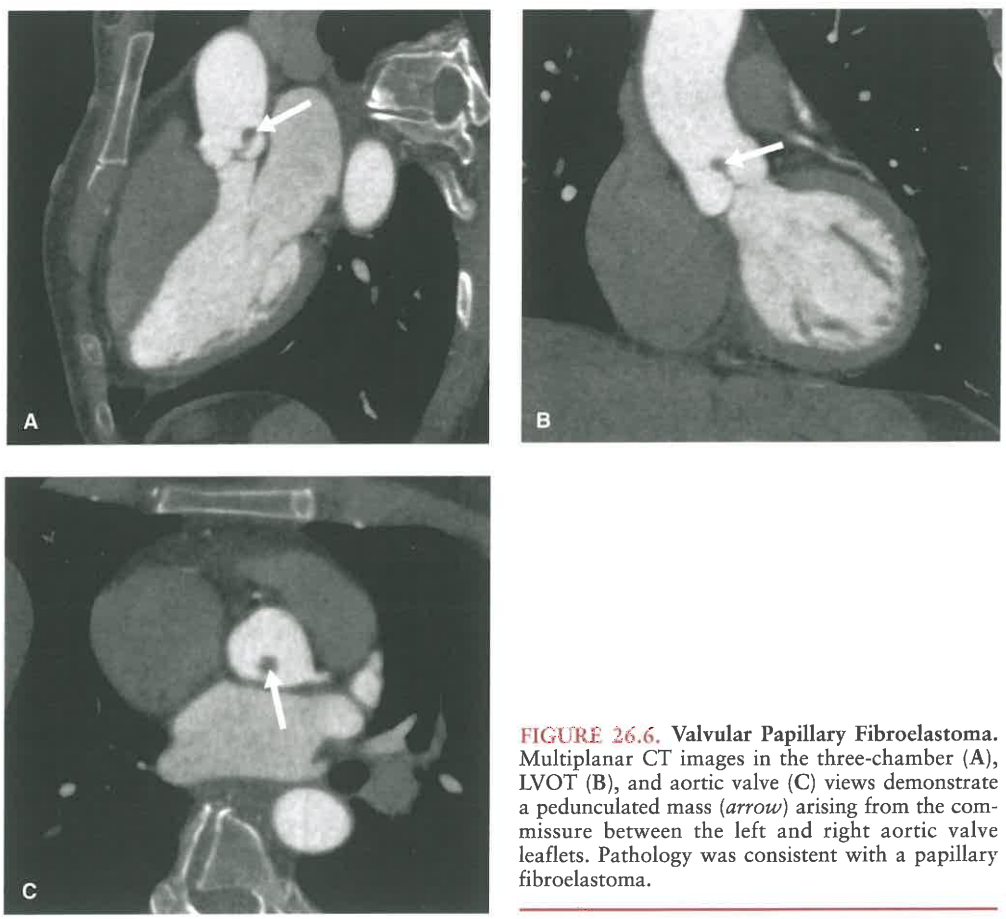

FIGURE 26.6. **Valvular Papillary Fibroelastoma.** Multiplanar CT images in the three-chamber (A), LVOT (B), and aortic valve (C) views demonstrate a pedunculated mass (*arrow*) arising from the commissure between the left and right aortic valve leaflets. Pathology was consistent with a papillary fibroelastoma.

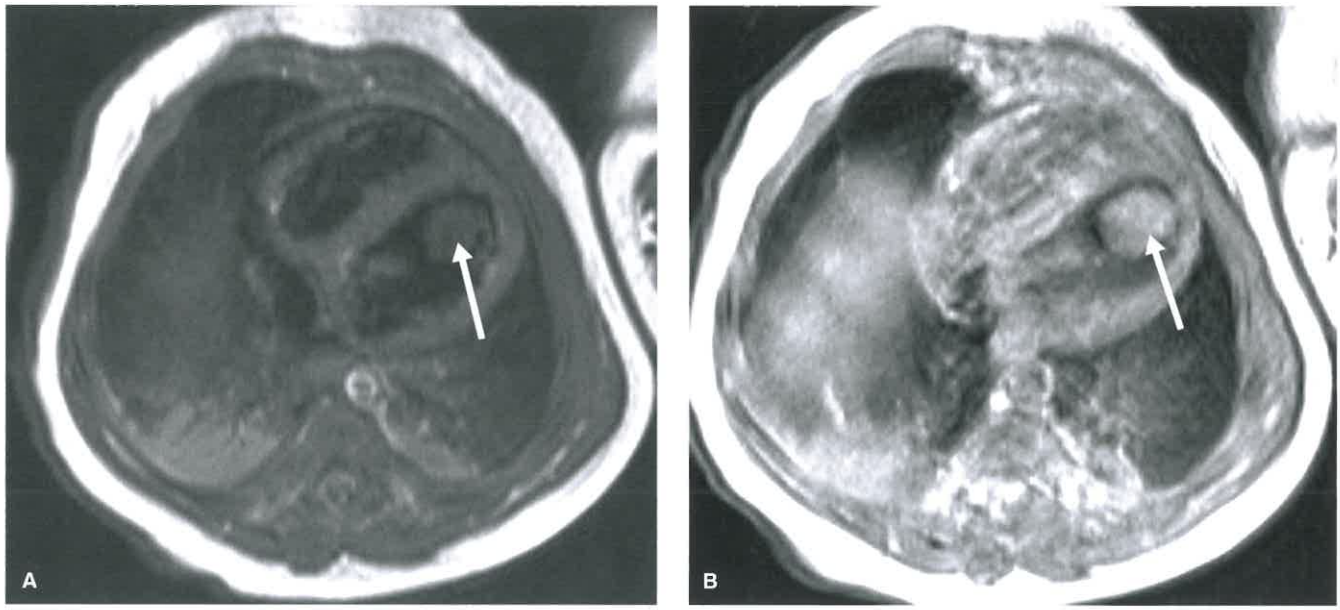

FIGURE 26.7. **Cardiac Rhabdomyoma.** Axial CMR T1W imaging (**A**) demonstrates a hypointense intracavitary mass (*arrow*) which demonstrates mild hyperintense signal (*arrow*) on the T2W sequences (**B**) in a newborn with known tuberous sclerosis.

fibrous tissue. The presence of delayed gadolinium enhancement is a key feature in distinguishing a fibroelastoma from a vegetation, which is the main differential diagnosis for a valvular mass. In general, while inflamed tissue surrounding a vegetation may enhance on delayed imaging, enhancement within a vegetation is usually mild or absent. In addition, as vegetations represent infected thrombi, there is often destruction of the associated valve with valvular or perivalvular regurgitation, which is absent with fibroelastoma. Lastly, patients with infective endocarditis are often febrile, septic, and the lungs may demonstrate subpleural cavitary nodules due to septic emboli. These findings are absent in fibroelastomas.

Rhabdomyoma. Cardiac rhabdomyomas are benign congenital tumors which are the most common primary tumors in infants and children. They account for 50% to 75% of pediatric cardiac tumors, equally affecting males and females. Rhabdomyomas are hamartomas of altered enlarged cardiac myocytes which arise as small intramural nodules in the ventricular myocardium, measuring between 1 and 3 cm on average. While these tumors may be solitary and occur in isolation, 50% of cases are seen in patients with tuberous sclerosis and are usually multiple. The presence of multiple cardiac rhabdomyomas has a 95% association with tuberous sclerosis, and almost all patients with this genetic disorder will have cardiac rhabdomyomas in infancy. The majority of cases are asymptomatic and many of the tumors will regress with age, usually before the age of 4. Occasionally, rhabdomyomas can cause in utero arrhythmias, or protrude into the ventricular chamber causing obstruction, heart failure, and intrauterine demise.

Most rhabdomyomas are detected on pre- or postnatal echocardiograms, seen as solid hyperechoic masses either within the ventricular myocardium or intracavitary and attached to the myocardium. Given that their attenuation is similar to normal myocardium, rhabdomyomas may be difficult to detect on CT but can appear as smooth, intramyocardial nodules. On MRI, they are isointense to normal myocardium on T1W images, mildly hyperintense on T2W images, and will demonstrate minimal to no hyperenhancement after administration of contrast (Fig. 26.7). The differential for a cardiac mass in a neonate or infant includes rhabdomyoma, fibroma, teratoma, and rhabdomyosarcoma. Rhabdomyomas can be differentiated by their multiplicity, homogeneous soft tissue signal, hyperintense signal on T2W sequences (as opposed to cardiac fibromas), and minimal to no enhancement.

Fibroma. Cardiac fibromas are benign fibrous hamartomas which are the second most common cardiac tumors in infants and children. About one-third of cases are found in infants before the age of 1, while 15% of cardiac fibromas are found in adolescents and adults. They are nonencapsulated fibrous tumors composed of neoplastic fibroblasts and abundant collagen. Fibromas are typically solitary, intramural tumors measuring between 2 and 7 cm. It may be a discrete mass or focal wall thickening, mimicking focal hypertrophy. The left ventricular wall or interventricular septum are common locations, with rarer cases found in the right atrium or ventricle. These tumors have an association with Gorlin syndrome (also termed basal cell nevus syndrome), an autosomal dominant syndrome of basal cell carcinoma, odontogenic keratocysts, and other neoplasms. One-half to two-thirds of the cardiac fibromas are symptomatic with a range of symptoms including chest pain, heart failure, arrhythmias, syncope, or sudden cardiac death.

On CT, fibromas will classically appear as a well-defined, homogeneous low attenuation mass located within the left ventricular myocardium. Coarse calcifications are present in 15% to 20% of cases and are often located centrally. After contrast, fibromas demonstrate mild enhancement on CT. On MRI, fibromas are usually isointense to the adjacent myocardium on T1W MR sequences, and hypointense on the T2W images due to their fibrous components. While fibromas are avascular and will show no enhancement during perfusion imaging, they will classically show intense enhancement with late gadolinium imaging due to their large amount of collagen creating an expanded extracellular space for contrast to pool into (Fig. 26.8). The differential diagnosis for an intramural myocardial lesion includes metastatic disease, rhabdomyoma (particularly in children), hemangioma, rhabdomyosarcoma, and focal hypertrophic cardiomyopathy which can mimic a mass. However, the combination of hypointense signal on the T2W

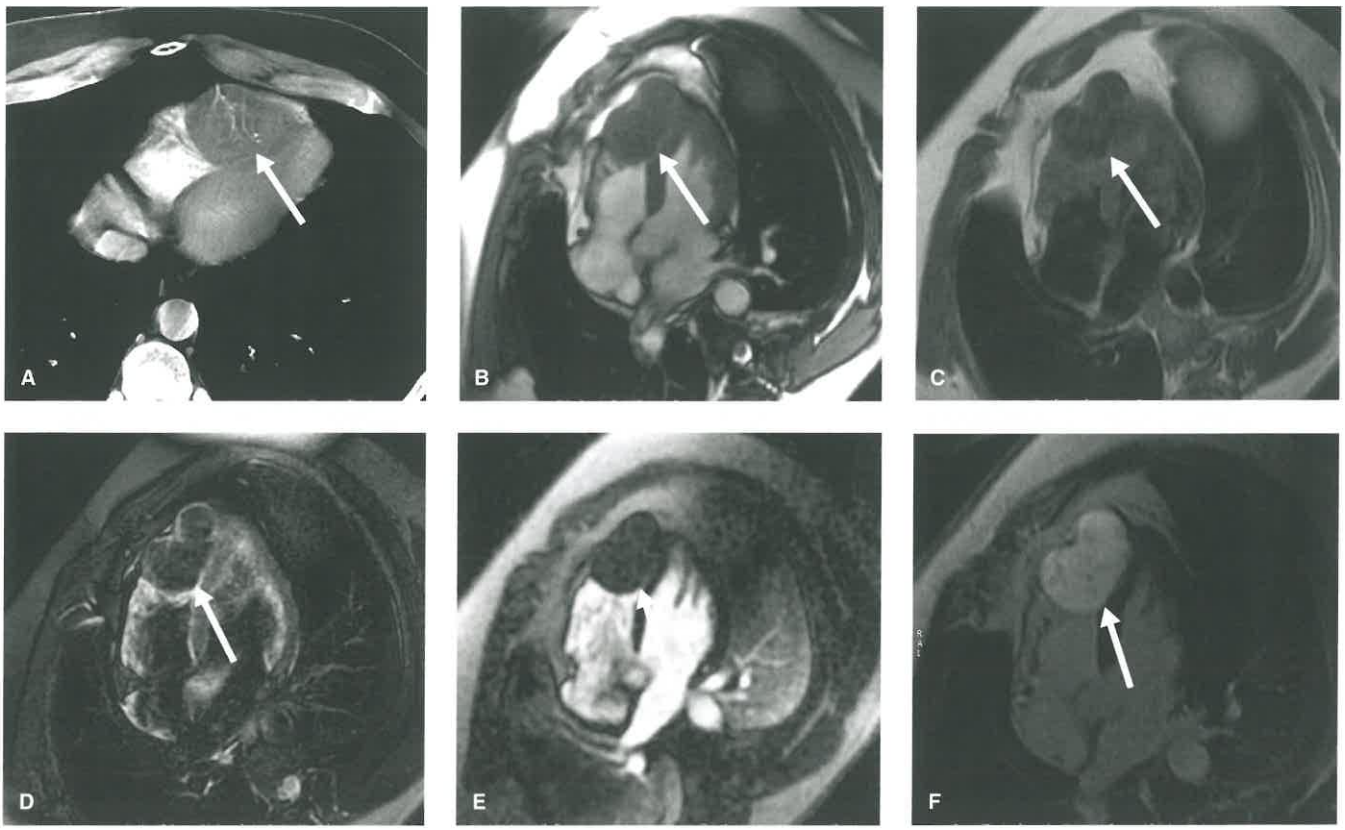

FIGURE 26.8. **Cardiac Fibroma.** Axial nongated postcontrast CT (**A**) demonstrates a large mass within the right ventricular apex (*arrow*) with several calcified foci. It demonstrates hypointense signal on T1W images (**B**), hypointense signal on T2W images (**C**) without and with fat saturation (**D**), lack of contrast enhancement during perfusion (**E**) indicating avascularity, and hyperintense homogeneous enhancement on LGE imaging (**F**). The diagnosis of cardiac fibroma was confirmed after surgical removal.

sequences and intense LGE is very uncommon in any other entity aside for a fibroma.

Hemangioma. Cardiac hemangiomas are rare tumors that account for 5% to 10% of all primary benign cardiac tumors. They are composed of vascular endothelial cells and can be arteriovenous, capillary, or cavernous in type. Fifty percent of cases are made up of the arteriovenous type, which is made up of dysplastic arterial and venous structures. Hemangiomas can be located in any part of the heart with 75% of cases being intramural. Intracavitary tumors are usually smaller and can be connected to the endocardium by a short stalk. Cardiac hemangiomas are commonly asymptomatic, although patients may present with dyspnea on exertion. There is an association with Kasabach–Merritt syndrome, which is characterized by multiple hemangiomas causing recurrent thrombocytopenia and consumptive coagulopathy.

On cardiac CT, hemangiomas are heterogeneous in density and will exhibit heterogeneous enhancement after contrast administration. Some cases may demonstrate internal calcifications. On MRI, they are heterogeneous and predominately hyperintense on both the T1W and T2W images. On both perfusion and delayed-phase imaging, the arteriovenous and capillary subtypes will demonstrate intense enhancement due to their vascular components, except in the areas of calcification (Fig. 26.9).

Paraganglioma. Cardiac paragangliomas are rare cardiac tumors derived from clustered neuroendocrine cells and are closely related to pheochromocytomas. They typically occur in adults during the third or fourth decades. Like any paraganglioma found within the body, they may produce catecholamines which can cause hypertension or other symptoms attributable to excess catecholamine production. Five percent to 10% of cardiac paragangliomas can be metastatic, with osseous involvement being the most common. Cardiac paragangliomas can be present in patients with the Carney triad, which is made up of extra-adrenal pheochromocytoma, gastrointestinal stromal tumor (GIST), and pulmonary chondroma (this is not to be confused with the Carney complex mentioned regarding cardiac myxomas). They most commonly occur in the left atrial wall, in the location of the normal cardiac paraganglioma cells, typically involving either the left atrial roof or posterior wall. Other reported locations include the interatrial septum or right atrium.

On both CT and MRI, cardiac paragangliomas will commonly show intense enhancement following contrast administration, both on the early- and delayed-phase imaging. Central necrosis and hemorrhage along with scattered internal calcification may be present as well. Paragangliomas are typically hypo- to isointense on T1W imaging and extremely hyperintense on T2W sequences (Fig. 26.10). Focal cardiac abnormal uptake on iodine-123 or iodine-131 metaiodobenzylguanidine (MIBG) scintigraphy is highly specific for cardiac paragangliomas as it is selectively taken up by extra-adrenal paragangliomas.

Other Benign Cardiac Neoplasms. Additional rare benign neoplasms include teratomas, lymphangiomas, and hamartomas. Cardiac teratomas are germ cell tumors made up of several different types of tissue and are like any other teratoma in the body. They are commonly found in infants/children as complex multilocular, heterogeneous cystic masses growing within the pericardial sac, typically on the right side. They are

FIGURE 26.9. **Cardiac Hemangioma.** Multiple cardiac MR images in the two-chamber view demonstrate an exophytic large mass (*arrow*) arising from the left ventricular apex which demonstrated iso- to mildly hyperintense signal on the SSFP (**A**) and T1W images (**B**), and intense enhancement on the postcontrast imaging (**C**). Findings were consistent with a hemangioma after surgical removal.

usually large in size and associated with a pericardial effusion. Teratomas will demonstrate calcification and fat and commonly exhibit an attachment to the aorta via a pedicle.

Cardiac lymphangiomas are benign abnormal collections of lymphatic vessels which are rare benign neoplasms, most commonly found in children. They are typically multiloculated cystic lesions within the pericardial space and may be associated with a chylous pericardial effusion. On CT, they appear as well-circumscribed lesions with varying degrees of attenuation values. On MRI, there may be areas of high signal intensity on the T1W images due to proteinaceous material within them. Lymphangiomas will also demonstrate hyperintense signal on T2W images due to their cystic spaces.

Cardiac hamartomas are extremely rare and are composed of hypertrophied disorganized myocytes with interstitial fibrosis. They most commonly occur within the left ventricular myocardium and will demonstrate enhancement on both CT and MRI. On MRI, hamartomas will demonstrate similar signal characteristics to the normal myocardium but will demonstrate avid enhancement on the early and delayed-phase imaging postcontrast administration (Fig. 26.11). Distinguishing hamartomas from the focal form of hypertrophic cardiomyopathy on imaging may be extremely difficult. These two entities will share some histologic features but can be distinguished by the lack of increased vascularity and more diffuse myocardial involvement seen with hypertrophic cardiomyopathy.

MALIGNANT CARDIAC TUMORS

Metastatic Disease

Metastatic disease involving the heart is the most common cardiac mass found in the adult population. It is approximately 20 to 40 times more common than all primary cardiac tumors and is associated with a poor prognosis. Approximately 10% of patients with primary malignancy have cardiac metastatic involvement, although this is often only visible on histopathology. Metastatic disease can involve the heart via a number of pathways including: hematogenous or lymphatic seeding from a tumor at a different site of the body, direct tumor invasion from an adjacent primary within the mediastinum or lungs, or transvenous intracavitary contiguous extension from the inferior vena cava (IVC), superior vena cava (SVC), or pulmonary veins. Lung cancer is the most common metastatic lesion to the heart accounting for 30% to 40% of cases followed by hematologic malignancies, breast cancer, and esophageal cancer. Direct

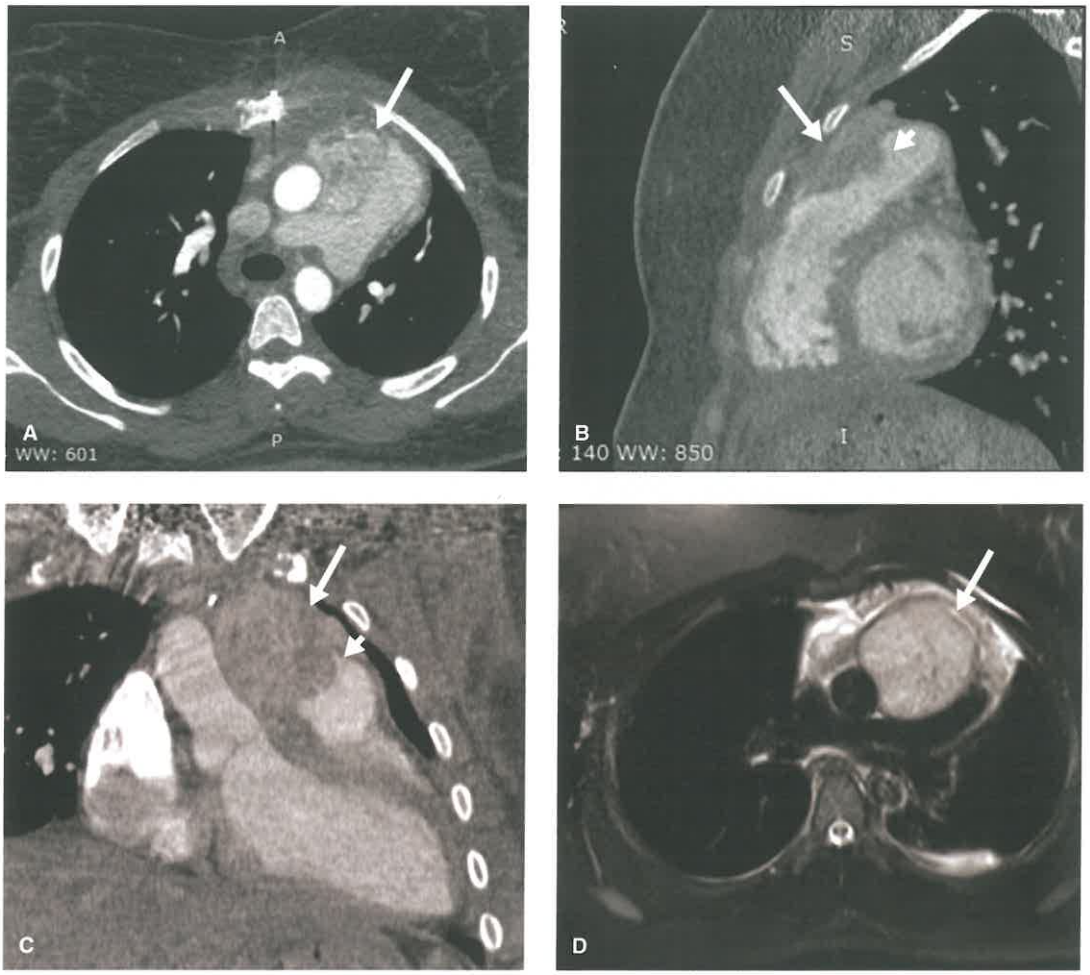

FIGURE 26.10. **Paraganglioma.** Axial postcontrast ECG-gated CT (**A**) demonstrates an avidly enhancing mediastinal mass situated between the ascending aorta and main pulmonary artery (*arrow*). Sagittal (**B**) and coronal (**C**) oblique CT-reconstructed images demonstrate invasion of the mass (*arrow*) into the right ventricular outflow tract (*arrowhead*). The lesion (*arrow*) demonstrates hyperintense signal on T2W fat-saturation MR axial images (**D**). Findings were consistent with a paraganglioma after surgical resection.

invasion or lymphatic extension to the pericardium and epicardium is the most common route of spread and is often accompanied by a malignant pericardial effusion. Melanomas, renal cell carcinomas, and sarcomas are the most common tumors to spread to the heart hematogenously and usually result in intramural involvement. Abdominal and pelvic malignancies can invade the IVC and grow superiorly into the right atrium.

While most cases of cardiac metastasis are clinically silent, symptoms usually manifest due to altered cardiac function, flow obstruction, or involvement of the electrical conduction system related to the location that is involved. Range of symptoms include syncope, left- or right-sided heart failure, arrhythmias, heart block, or significant pericardial effusions that can lead to cardiac tamponade. Obstructive symptoms are commonly seen in transvenous extension of disease, with involvement of the SVC/IVC and right atrium.

When imaging the heart for metastatic disease, the most common findings will include pericardial involvement and/or intracavitary masses. Many cases of cardiac metastatic disease will have an associated malignant pericardial effusion. Echocardiography is the best initial evaluation for pericardial involvement, specifically to evaluate for an effusion, its effect on cardiac function, and assessment for tamponade physiology. While echocardiography may demonstrate pericardial thickening or nodularity, it does not evaluate the entire pericardium and may not detect pericardial deposits. Please refer to Chapter 29 on pericardial disease.

Both CT and MRI will provide a broader anatomic evaluation of the heart in assessing for metastatic disease, as they are able to evaluate the entire heart as well as its surrounding structures. Metastatic involvement of the myocardium will present on CT/MRI as a discrete mass or masses. CT is the best modality to evaluate for lung cancer invasion into the pulmonary veins and is excellent at assessing for invasion of abdominal tumors into the IVC and right atrium. While a routine contrast enhancement CT may detect cardiac metastases, ECG gating should be considered if there is concern for cardiac involvement. The presence of heterogeneous enhancement on CT will help distinguish tumor thrombus from bland thrombus which is a frequent clinical dilemma.

As with primary cardiac masses, CMR will offer superior tissue characterization of cardiac metastatic disease and will provide excellent functional and hemodynamic assessment. In general, metastatic lesions will demonstrate low signal on T1W images and high signal on T2W images. Melanoma or hemorrhagic lesions may demonstrate high signal on the T1W

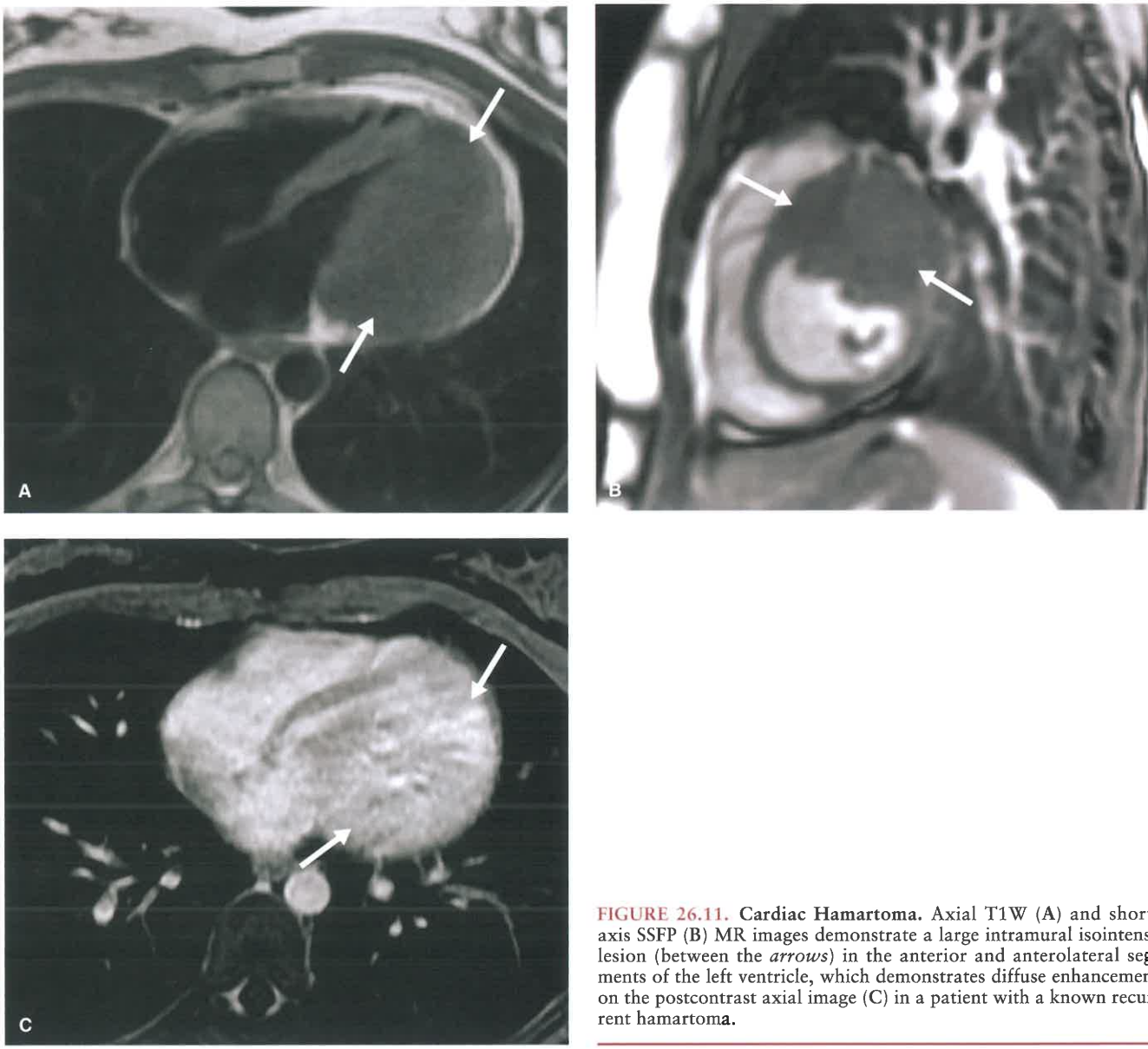

FIGURE 26.11. **Cardiac Hamartoma.** Axial T1W (A) and short-axis SSFP (B) MR images demonstrate a large intramural isointense lesion (between the *arrows*) in the anterior and anterolateral segments of the left ventricle, which demonstrates diffuse enhancement on the postcontrast axial image (C) in a patient with a known recurrent hamartoma.

images as well. These lesions will generally demonstrate heterogeneous enhancement, which may not be clearly detected on postcontrast CT images (Fig. 26.12). Due to its ability to detect subtle metastatic foci, MRI is superior to CT for accurate extent of disease evaluation. In addition, delayed enhancement imaging with a long inversion time (TI = 600) allows for differentiation of tumor from thrombus, as the prolonged inversion time selectively nulls avascular tissue. Therefore, thrombus will be hypointense on the long inversion time images, while enhancing tumor will demonstrate hyperintense signal.

Sarcoma. Primary cardiac sarcomas are neoplastic lesions which arise from the mesenchymal cells within the cardiac muscle. They are the most common primary malignant tumor of the heart, accounting for one-third of cases and include several subtypes (Table 26.4). Angiosarcoma is the most common differentiated cardiac sarcoma, compromising nearly 40% of cases. Undifferentiated sarcomas are the second most common sarcoma involving the heart, making up 25% of cases. Rhabdomyosarcoma is the most common primary cardiac malignancy in childhood and accounts for 4% to 7% of all cardiac sarcomas. Other types of primary cardiac sarcomas include leiomyosarcoma, osteosarcoma, and fibrosarcoma.

Cardiac sarcomas primarily affect adults between the third and fifth decades and are extremely rare in children. They carry a poor prognosis with mean survival ranging from 3 months to 4 years. At presentation, many cases exhibit evidence of metastatic disease, frequently involving the lungs. Dyspnea is the common symptom, with other presentations including chest pain, arrhythmias, tamponade, and/or death.

Typical locations and imaging appearances of cardiac sarcomas vary based on the histologic subtype. They may be intramural with infiltration and thickening of the myocardium and/or intracavitary, and will commonly demonstrate components of hemorrhage and necrosis. Pericardial involvement with a hemorrhagic pericardial effusion and nodular thickening

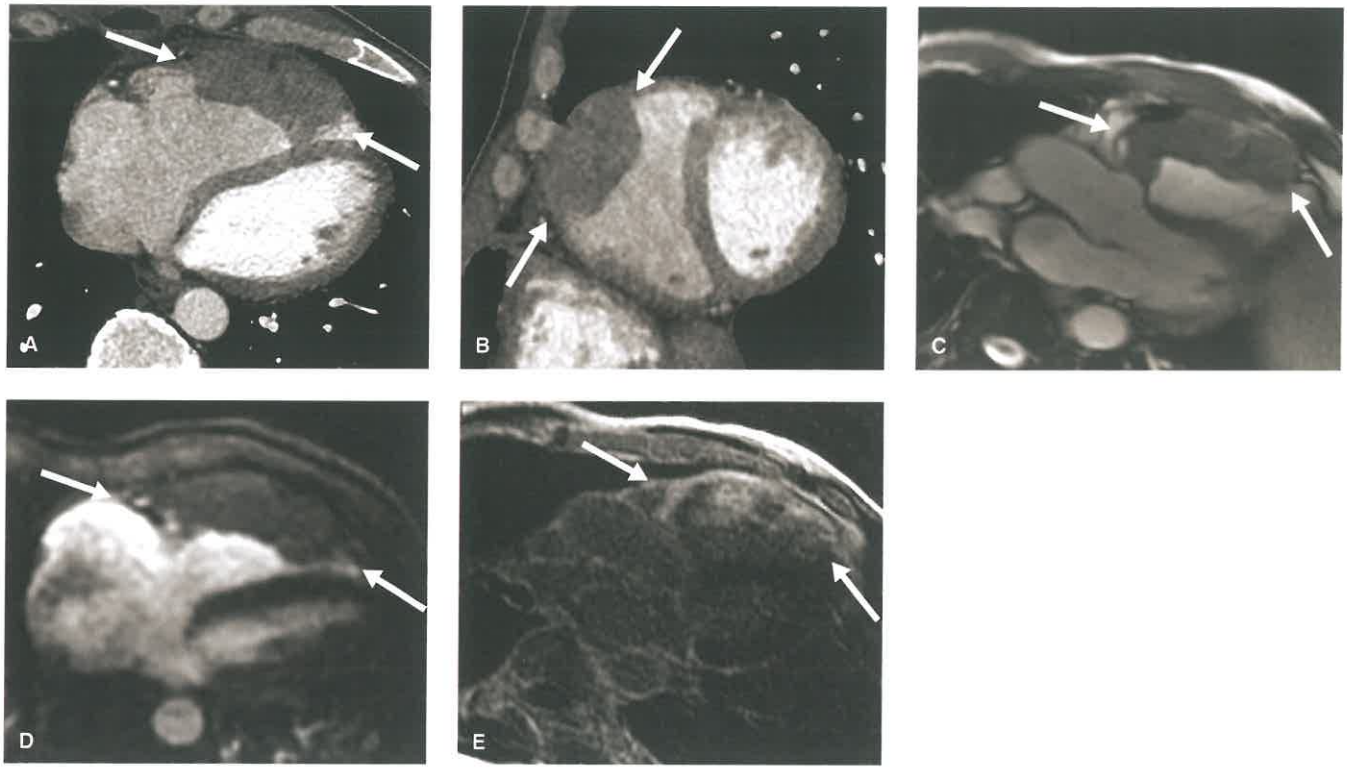

FIGURE 26.12. **Cardiac Metastasis.** Postcontrast nongated CT in the axial (**A**) and short-axis (**B**) planes, in a patient with known metastatic lung cancer, demonstrates an infiltrative mass (between the *arrows*) in the free wall of the right ventricle. It demonstrates hypo- to isointense signal in relation to the myocardium on the SSFP sequence (**C**) and heterogeneous enhancement on the perfusion (**D**) and late gadolinium engagement (**E**) images.

of the pericardium is another common feature. Invasion into the mediastinum or valvular destruction may be present.

Cardiac angiosarcoma is the only cardiac sarcoma that predominately arises in the right atrium in the region of the right atrioventricular groove. While there may be a discrete right atrial mass, tumor can often be seen extending anteriorly along the wall of the right atrium and right ventricle. Encasement of the right coronary artery is a common finding. On both CT and MRI, they appear as heterogeneous soft tissue masses with areas of necrosis. A characteristic finding is intense enhancement within the soft tissue component of the tumor and rapid enhancement on first-pass perfusion (Fig. 26.13). The main differential for an infiltrative mass in the region of the right atrioventricular groove is metastatic disease or lymphoma.

While angiosarcomas predominate in the right atrium and rhabdomyosarcoma have no chamber predilection, the other histologic subtypes of cardiac sarcomas usually occur in the left atrium. They present as large masses that infiltrate along the wall of the left atrium. As they crawl and invade along the left atrial wall, they often invade and obstruct the pulmonary veins and/or the mitral annulus. Although myxomas—which are the most common primary cardiac tumor—also occur in the left atrium, they are not infiltrative and do not invade into the pulmonary veins. In addition, the vast majority of left atrial myxomas occur along the interatrial septum in the region of the fossa ovalis, a finding that is not seen with left atrial sarcomas. Like other aggressive tumors, left atrial sarcomas appear as heterogeneous soft tissue masses, often with areas of necrosis. Enhancement is usually present but is often not as pronounced as with right atrial angiosarcomas. In general, it is often difficult to differentiate between the histologic subtypes of cardiac sarcoma on imaging, although prominent osteoid matrix in a large left atrial mass should raise the suspicion for a cardiac osteosarcoma.

Lymphoma. Primary cardiac lymphoma is defined as lymphoma exclusively involving the heart and/or pericardium. It is usually of the non-Hodgkin B-cell type, most commonly occurring in immunocompromised patients, often related to infection with the Epstein–Barr virus. Others more susceptible to primary cardiac lymphoma include posttransplant patients or those with HIV/AIDS. It is quite rare, making up 1.3% of primary cardiac tumors and only 0.5% of extranodal lymphomas at autopsy. Secondary cardiac lymphoma due to systemic lymphoma involving the heart is more common, with one study showing approximately 30% of patients with lymphoma having cardiac involvement at autopsy. Primary cardiac lymphoma commonly involves the right side of the heart, particularity the right atrium and has a predilection for the right atrioventricular groove similar to angiosarcoma. Most common clinical presentation includes arrhythmias including atrioventricular block, heart failure, dyspnea, or a pericardial effusion.

On cross-sectional imaging, primary cardiac lymphoma will manifest as an ill-defined, infiltrative epicardial or myocardial mass, or multiple masses usually along the right side of the heart, with an associated pericardial effusion. The right atrium is most commonly involved, followed by the

TABLE 26.4

SUMMARY OF CARDIAC SARCOMA SUBTYPES AND THEIR IMAGING FEATURES

CARDIAC SARCOMA SUBTYPES	MALIGNANT CARDIAC TUMORS (%)	COMMON TUMOR LOCATION	IMAGING AND OTHER FEATURES
Angiosarcoma	37–40	Right atrium	■ Two morphologic types: 1. Well-defined mass protruding into the right atrium 2. Diffusely infiltrating mass along the right side of the heart ■ Has a propensity for hemorrhage and necrosis ■ Commonly has pericardial invasion and a hemorrhagic pericardial effusion
Undifferentiated sarcoma	24–33	Left atrium	■ May be a discrete mass or an irregular infiltrative lesion ■ Commonly hemorrhagic
Leiomyosarcoma	8–10	Posterior wall of the left atrium or IVC	■ Sessile lobulated hypodense mass on CT ■ May be multifocal ■ May arise or invade into the pulmonary veins
Osteosarcoma	3–9	Left atrium	■ Typically large tumors which are centered in the left atrium, unlike osteosarcoma metastases to the heart ■ Commonly contain large foci of calcification
Rhabdomyosarcoma	4–7	No chamber predilection	■ Most common primary malignant tumor in children, but can affect all ages ■ May be solitary or multifocal intramural masses
Liposarcoma	<1%	Left or right atrium	■ May show foci of fat density on CT ■ On MRI, fat-saturation sequences are not particularly helpful unlike cardiac lipoma or lipomatous hypertrophy of the interatrial septum

right ventricle and then the left-sided chambers. A unique feature of lymphoma is its tendency to extend along the epicardium, encasing adjacent structures including the coronary arteries, aortic root, or pulmonary vessels. In addition, it may diffusely involve the myocardium, masquerading as myocardial hypertrophy or it can demonstrate nodular or lobulated intracavitary components. The lesion will usually be hypo- to isodense to the surrounding myocardium on CT with heterogeneous enhancement, postcontrast administration. CMR best depicts the extent of the myocardial and pericardial involvement due to its better tissue characterization. On MRI, it will demonstrate isointense signal to the myocardium on T1W images, hyperintense signal on T2W images, and variable enhancement postcontrast (Fig. 26.14). Differential diagnosis for an ill-defined infiltrative lesion along the epicardial surface includes metastatic disease or sarcomas. Lymphoma may be distinguished from these entities by their homogeneous signal throughout the lesion. This homogeneous signal in cardiac lymphoma is due to the absence of necrosis or hemorrhage, which causes the variable signal demonstrated in metastatic lesions and sarcoma. When solely within the myocardium, it can be mistaken for hypertrophic cardiomyopathy and when intracavitary, it may be confused for a thrombus or myxoma.

Tumorlike Lesions

Thrombus. Intracardiac thrombus is the most common intracardiac lesion and can involve any cardiac chamber. In the right atrium and right ventricle, thrombi are commonly attached to intravascular catheters/lines or are the sequelae of deep venous thrombosis with subsequent embolization. In atrial fibrillation, thrombus will usually form in the left atrial appendage due to poor blood flow, while in the setting of ventricular dysfunction it will form in akinetic or aneurysmal portions of the ventricle, often in the left ventricular apex.

Differentiating thrombus from other cardiac lesions is a frequent diagnostic question. While postcontrast cardiac CT imaging is an excellent tool for detecting and localizing intracavitary thrombi, it is limited in differentiating thrombus from tumor. Thrombus is hypodense on CT and does not enhance. Given this, thrombus is often best delineated during the portal venous phase of imaging where it appears hypodense to

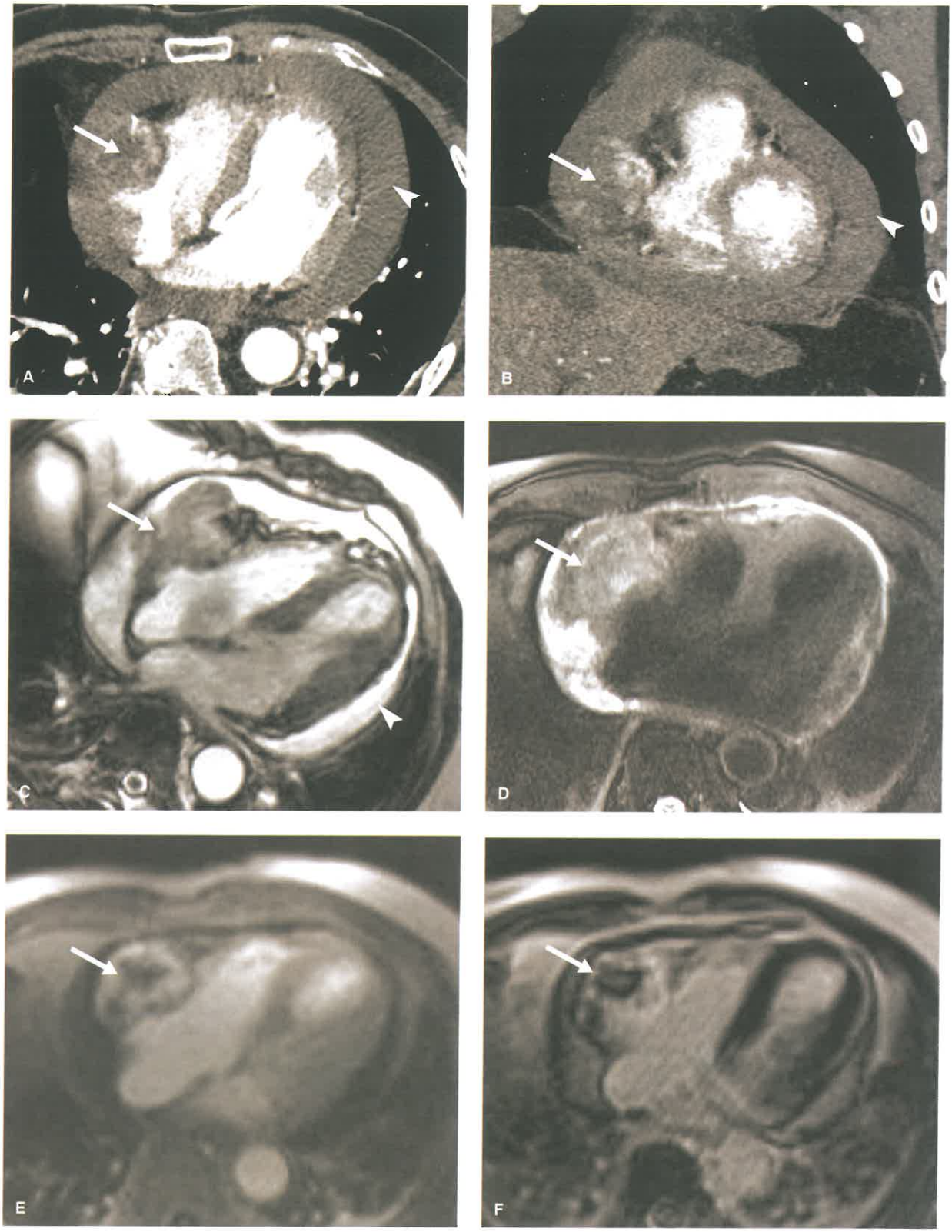

FIGURE 26.13. **Cardiac Angiosarcoma.** Axial (**A**) and coronal (**B**) postcontrast CT images demonstrate a heterogeneous enhancing mass in the right atrioventricular groove (*arrow*) with a pericardial effusion (*arrowhead*). CMR shows a heterogeneous hyperintense lesion on the SSFP (**C**) and T2W images (**D**) with avid enhancement on both the perfusion (E) and LGE (F) sequences. The central nonenhancing area within the mass represents necrosis.

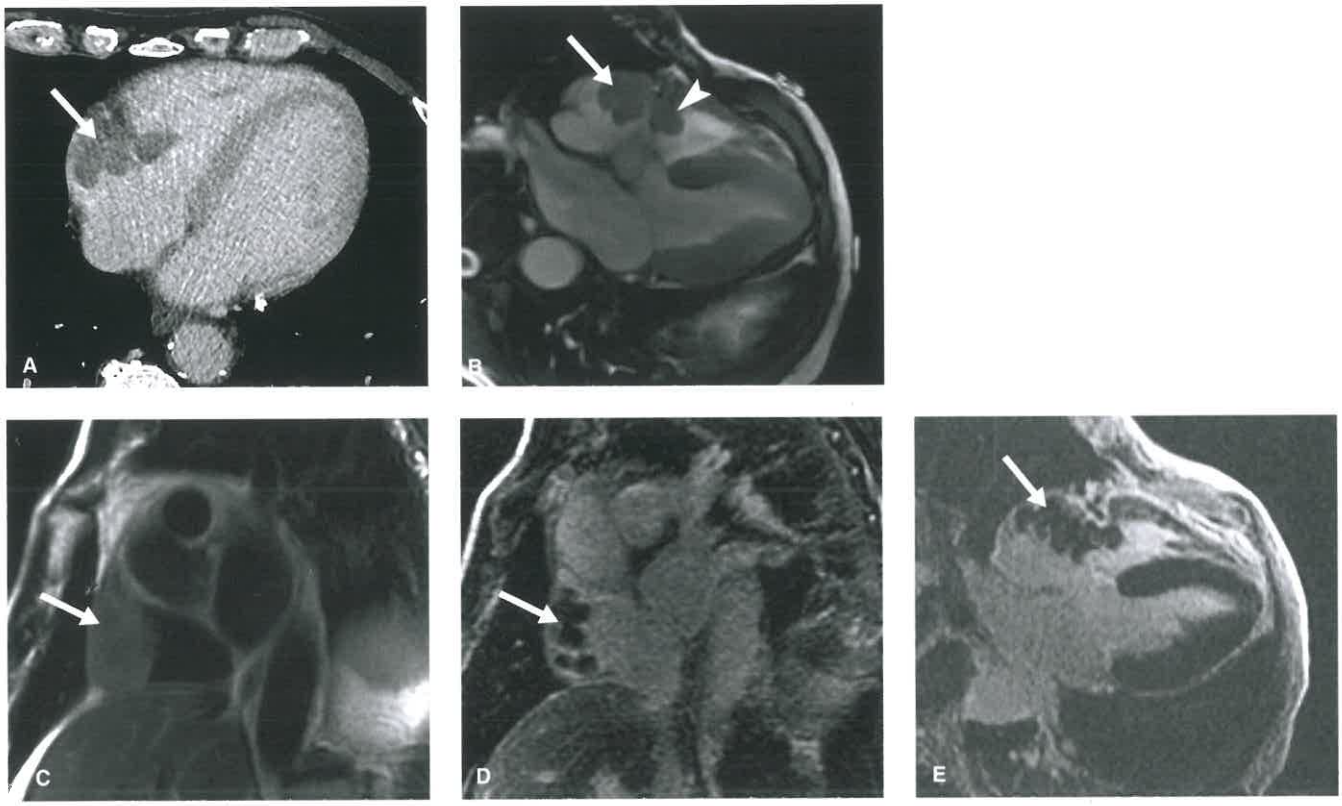

FIGURE 26.14. **Cardiac Lymphoma.** Postcontrast axial CT (**A**) and MR SSFP imaging in the four-chamber view (**B**) demonstrate a multilobulated mass (*arrow*) in the right atrium extending along the lateral aspect into the right ventricle (*arrowhead*). It demonstrates isointense signal on the T2W images and minimal to no enhancement on LGE images. Biopsy results were consistent with B-cell lymphoma.

the normally enhancing myocardium. CMR is the imaging of choice in distinguishing thrombus from tumor. Imaging characteristics of thrombus change with its age, with acute thrombus demonstrating hyperintense signal on T1W and T2W sequences and chronic thrombus demonstrating hypointense signal on both sequences. Subacute thrombus will be hyperintense on T1W images and hypointense on T2W images. Thrombus will characteristically show no contrast uptake on first-pass perfusion or T1W postcontrast images. Importantly, thrombus will demonstrate dark signal on delayed enhancement sequences with a long inversion time of 600 ms (Fig. 26.15) and at times more intermediate signal using a standard inversion time of 300 ms, a finding that is absent in most tumors. One recent study has shown that performing a dedicated TI scout ("Look–Locker") sequence through the mass can distinguish the two entities, as thrombus demonstrated a typical pattern of hyper/isointensity with a short inversion time and hypointensity with long inversion time in 94% of cases, with only 2% of tumors demonstrating the same signal pattern. Of note, chronic organised thrombus may demonstrate peripheral enhancement on late gadolinum enhancement imaging due to fibrous material forming around it.

Lipomatous Hypertrophy of the Interatrial Septum. Lipomatous hypertrophy is a benign process characterized by proliferation of adipose cells within the interatrial septum. It occurs in up to 8% of the population and can be associated with an increased body mass index and large amounts of epicardial fat. The amount of fat usually will increase with age. The fat within the atrial septum is made up of mature unencapsulated adipose tissue resembling brown fat and can be metabolically active on FDG-PET. Most cases are incidentally discovered and are asymptomatic, with very rare cases causing supraventricular arrhythmias and sudden death.

Cross-sectional imaging will demonstrate a dumbbell-shaped fatty mass in the interatrial septum, commonly with asymmetric enlargement of its posterolateral component. The dumbbell shape is created by the sparing of the fossa ovalis. On MRI, the lesion will follow normal fat characteristics with both hyperintense signal on T1W and T2W sequences and loss of signal with fat-suppression techniques (Fig. 26.16). Normal septal thickness measures less than 1 cm, with cases of lipomatous hypertrophy measuring greater than 2 cm. Cases measuring up to 7 cm have been described as well. Cardiac lipoma is the main differential diagnosis and will have a true fibrous capsule. Sparing of the fossa ovalis is a key feature in lipomatous hypertrophy that helps in distinguishing it from other abnormalities.

Vegetations. Valvular vegetations are adherent lesions made up of platelets, fibrin, and inflammatory cells that seed the valvular leaflets, usually in an area of endocardial injury. In infective endocarditis, these lesions are also composed of microorganisms, either bacterial or fungal. Noninfective endocarditis is rare and can be due to nonbacterial thrombotic endocarditis (NBTE) seen in the setting of malignancy or Libman–Sacks endocarditis which occurs in patients with systemic lupus erythematosus (SLE) due to deposition of immune complexes. The vegetations are irregular or rounded in shape, measuring a few millimeters to greater than 1 cm. Differential diagnosis includes papillary fibroelastoma, with infective endocarditis usually leading to leaflet destruction as opposed to papillary fibroelastoma which is a benign entity.

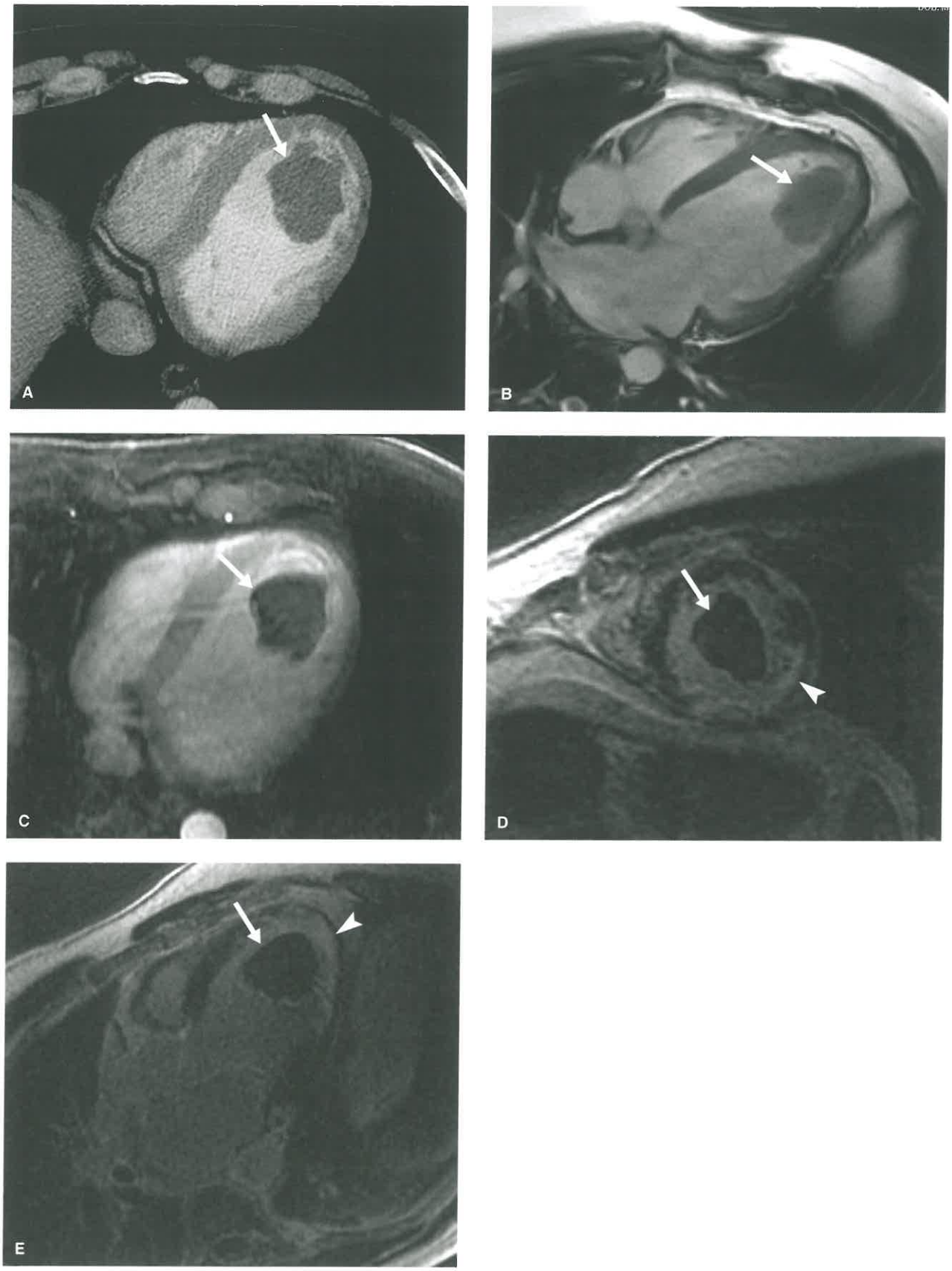

FIGURE 26.15. **Interventricular Thrombus.** Postcontrast nongated axial CT (**A**) and SSFP MR (**B**) images demonstrate a hypodense/hypointense lesion in the apical cavity of the left ventricle (*arrow*). It demonstrates no enhancement on the early post contrast images (**C**) and the LGE images in the short-axis (**D**) and three-chamber (**E**) views, although the left ventricular apical myocardium does demonstrate late gadolinium enhancement (*arrowhead*). Findings are consistent with an apical myocardial infarct and interventricular thrombus.

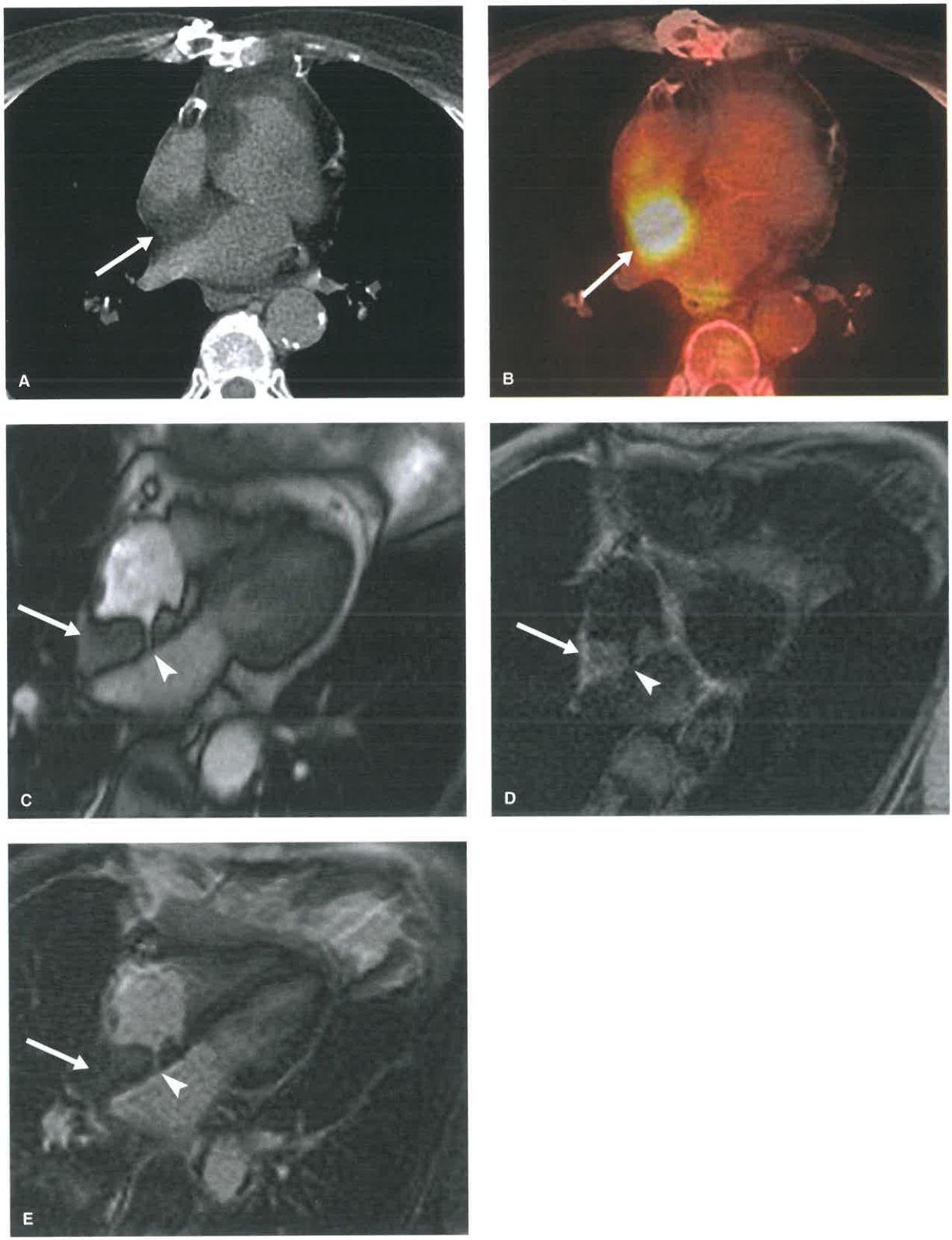

FIGURE 26.16. **Lipomatous Hypertrophy of the Interatrial Septum.** Axial CT (**A**) demonstrates a low-density lesion in the interatrial septum (*arrow*) which is FDG avid on a PET-CT due to the presence of brown fat (**B**). Follow-up CMR shows a lesion within the interatrial septum on the SSFP (**C**) image, which spares the fossa ovalis (*arrowhead*) and demonstrates hyperintense signal on T1W (**D**) and no LGE (**E**).

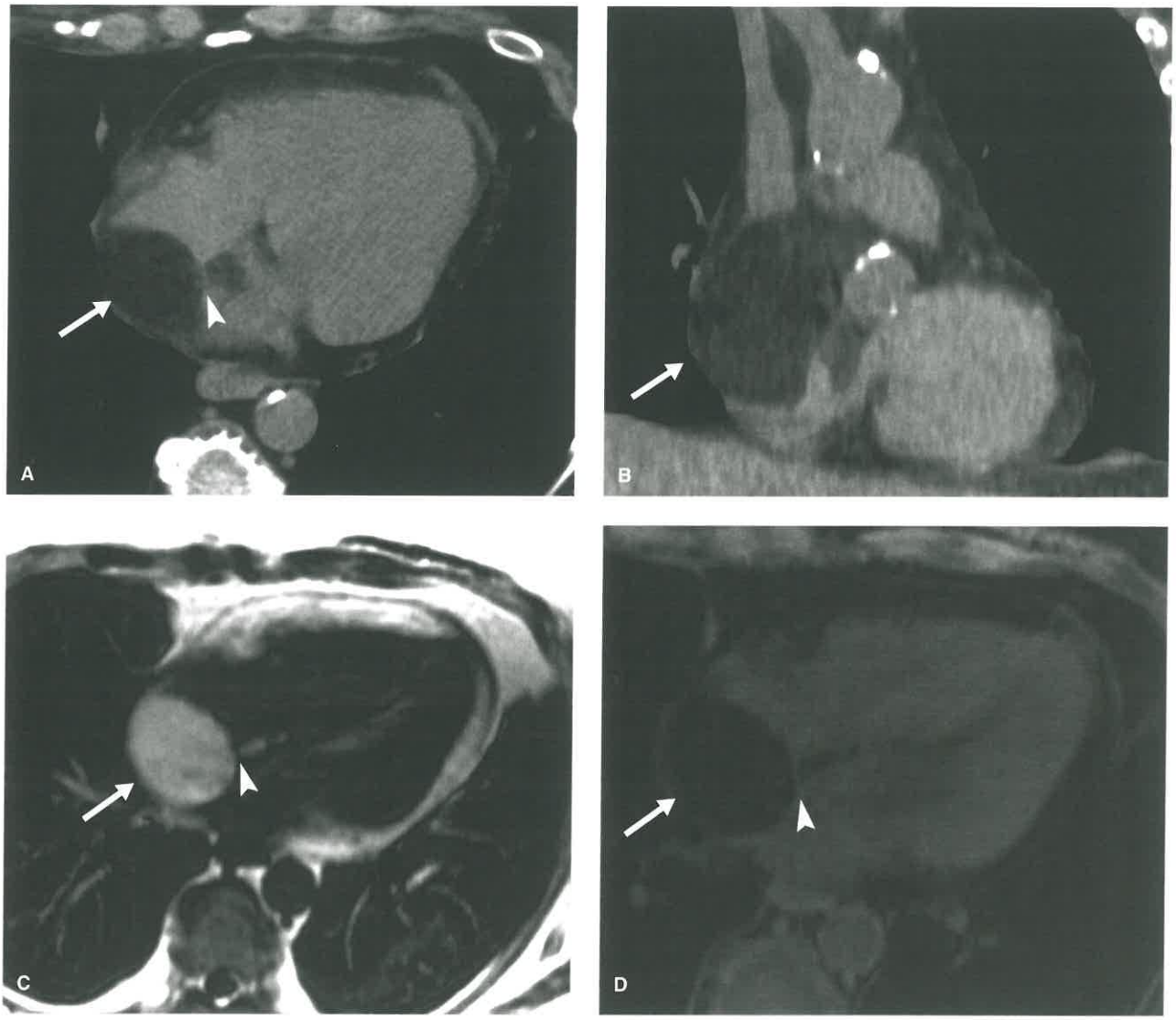

FIGURE 26.17. **Large Lipomatous Hypertrophy of the Interatrial Septum.** Noncontrast CT in the four-chamber (**A**) and coronal oblique (**B**) views demonstrates a large lesion in the interatrial septum measuring fat density (*arrow*), which spares the fossa ovalis (*arrowhead*), in a patient with a known supraventricular tachycardia. The lesion demonstrates homogenous hyperintense signal on the T1W images without fat suppression (**C**) and complete dropout of signal on the T1W images with fat suppression (**D**), consistent with fat.

Normal Anatomic Structures. Several normal anatomic structures may appear as pseudomasses on echocardiography but which are commonly distinguished from true pathology on cross-sectional imaging. The two most common structures are the crista terminalis and the eustachian valve. The crista terminalis is a normal anatomic structure which demarcates the area of embryologic fusion of the primitive right atrium and the sinus venosus. It is a vertically oriented smooth muscle ridge within the right atrium, which extends from the SVC to the IVC. The eustachian valve is a normal ridge of tissue at the junction of the right atrium and IVC, which in utero directed blood flow from the IVC into the fossa ovalis.

Suggested Readings

American College of Radiology. *ACR Manual on Contrast Media. Version 10.3.* Reston, VA: ACR; 2017.

Araoz PA, Mulvagh SL, Tazelaar HD, Julsrud PR, Breen JF. CT and MR imaging of benign primary cardiac neoplasms with echocardiographic correlation. *Radiographics* 2000;20(5):1303–1319.

Asopa S, Patel A, Khan OA, Sharma R, Ohri SK. Non-bacterial thrombotic endocarditis. *Eur J Cardiothorac Surg* 2007;32:696–701.

Bader RS, Chitayat D, Kelly E, et al. Fetal rhabdomyoma: prenatal diagnosis, clinical outcome, and incidence of associated tuberous sclerosis complex. *J Pediatr* 2003;143:620–624.

Becker AE. Primary heart tumors in the pediatric age group: a review of salient pathologic features relevant for clinicians. *Pediatr Cardiol* 2000;21(4): 317–323.

Beghetti M, Gow RM, Haney I, Mawson J, Williams WG, Freedom RM. Pediatric primary benign cardiac tumors: a 15-year review. *Am Heart J* 1997; 134:1107–1114.

Beghetti M, Prieditis M, Rabeyka IM, Mawson J. Images in cardiovascular medicine. Intrapericardial teratoma. *Circulation* 1998;97:1523–1524.

Bergey PD, Axel L. Focal hypertrophic cardiomyopathy simulating a mass: MR tagging for correct diagnosis. *AJR Am J Roentgenol* 2000;174(1): 242–244.

Beroukhim RS, Prakash A, Buechel ER, et al. Characterization of cardiac tumors in children by cardiovascular magnetic resonance imaging: a multicenter experience. *J Am Coll Cardiol* 2011;58:1044–1054.

Buckley O, Madan R, Kwong R, Rybicki FJ, Hunsaker A. Cardiac masses, part 1: imaging strategies and technical considerations. *AJR Am J Roentgenol* 2011a;197(5):W837–W841.

Buckley O, Madan R, Kwong R, Rybicki FJ, Hunsaker A. Cardiac masses, part 2: key imaging features for diagnosis and surgical planning. *AJR Am J Roentgenol* 2011b;197:W842–W851.

Burke AP, Rosado-de-Christenson M, Templeton PA, Virmani R. Cardiac fibroma: clinicopathologic correlates and surgical treatment. *J Thorac Cardiovasc Surg* 1994;108:862–870.
Burke AP, Virmani R. Cardiac myxoma: a clinicopathologic study. *Am J Clin Pathol* 1993;100:671–680.
Burke A, Virmani R. Tumors of the heart and great vessels. In: *Atlas of Tumor Pathology, 3rd Series, Fascicle 16*. Washington, DC: Armed Forces Institute of Pathology; 1996.
Bussani R, De-Giorgio F, Abbate A, Silvestri F. Cardiac metastases. *J Clin Pathol* 2007;60:27–34.
Carson W, Chiu SS. Image in cardiovascular medicine. Eustachian valve mimicking intracardiac mass. *Circulation* 1998;97:2188.
Chiles C, Woodard PK, Gutierrez FR, Link KM. Metastatic involvement of the heart and pericardium: CT and MR imaging. *Radiographics* 2001;21: 439–449.
Chun EJ, Choi SI, Jin KN, et al. Hypertrophic cardiomyopathy: assessment with MR imaging and multidetector CT. *Radiographics* 2010;30(5):1309–1328.
Cina SJ, Smialek JE, Burke AP, Virmani R, Hutchins GM. Primary cardiac tumors causing sudden death: a review of the literature. *Am J Forensic Med Pathol* 1996;17:271–281.
Dell'Amore A, Lanzanova G, Silenzi A, Lamarra M. Hamartoma of mature cardiac myocytes: case report and review of the literature. *Heart Lung Circ* 2011;20:336–340.
Edwards FH, Hale D, Cohen A, Thompson L, Pezzella AT, Virmani R. Primary cardiac valve tumors. *Ann Thorac Surg* 1991;52(5):1127–1131.
Fan CM, Fischman AJ, Kwek BH, Abbara S, Aquino SL. Lipomatous hypertrophy of the interatrial septum: increased uptake on FDG PET. *AJR Am J Roentgenol* 2005;184:339–342.
Ghadimi Mahani M, Lu JC, Rigsby CK, Krishnamurthy R, Dorfman AL, Agarwal PP. MRI of pediatric cardiac masses. *AJR Am J Roentgenol* 2014; 202:971–981.
Goldberg AD, Blankstein R, Padera RF. Tumors metastatic to the heart. *Circulation* 2013;128:1790–1794.
Gowda RM, Khan IA, Nair CK, Mehta NJ, Vasavada BC, Sacchi TJ. Cardiac papillary fibroelastoma: a comprehensive analysis of 725 cases. *Am Heart J* 2003;146:404–410.
Goyal P, Weinsaft JW. Cardiovascular magnetic resonance imaging for assessment of cardiac thrombus. *Methodist Debakey Cardiovasc J* 2013;9(3):132–136.
Grebenc ML, Rosado de Christenson ML, Burke AP, Green CE, Galvin JR. Primary cardiac and pericardial neoplasms: radiologic-pathologic correlation. *Radiographics* 2000;20:1073–1103.
Grebenc ML, Rosado de Christenson ML, Green CE, Burke AP, Galvin JR. Cardiac myxoma: imaging features in 83 patients. *Radiographics* 2002;22:673–689.
Grizzard JD, Ang GB. Magnetic resonance imaging of pericardial disease and cardiac masses. *Magn Reson Imaging Clin N Am* 2007;15:579–607.
Hamidi M, Moody JS, Weigel TL, Kozak KR. Primary cardiac sarcoma. *Ann Thorac Surg* 2010;90(1):176–181.
Hamilton BH, Francis IR, Gross BH, et al. Intrapericardial paragangliomas (pheochromocytomas): imaging features. *AJR Am J Roentgenol* 1997;168: 109–113.
Hananouchi GI, Goff WB 2nd. Cardiac lipoma: six-year follow-up with MRI characteristics, and a review of the literature. *Magn Reson Imaging* 1990; 8(6):825–828.
Heyer CM, Kagel T, Lemburg SP, Bauer TT, Nicolas V. Lipomatous hypertrophy of the interatrial septum: a prospective study of incidence, imaging findings, and clinical symptoms. *Chest* 2003;124:2068–2073.
Hoey ET, Mankad K, Puppala S, Gopalan D, Sivananthan MU. MRI and CT appearances of cardiac tumours in adults. *Clin Radiol* 2009;64:1214–1230.
Jeudy J, Kirsch J, Tavora F, et al. From the radiologic pathology archives: cardiac lymphoma: radiologic-pathologic correlation. *Radiographics* 2012;32(5): 1369–1380.
Kaji T, Takamatsu H, Noguchi H, et al. Cardiac lymphangioma: case report and review of the literature. *J Pediatr Surg* 2002;37:E32.
Kassop D, Donovan MS, Cheezum MK, et al. Cardiac masses on cardiac CT: a review. *Curr Cardiovasc Imaging Rep* 2014;7:9281.
Lembcke A, Meyer R, Kivelitz D, et al. Images in cardiovascular medicine: papillary fibroelastoma of the aortic valve: appearance in 64-slice spiral computed tomography, magnetic resonance imaging, and echocardiography. *Circulation* 2007;115:e3–e6.
Luna A, Ribes R, Caro P, Vida J, Erasmus JJ. Evaluation of cardiac tumors with magnetic resonance imaging. *Eur Radiol* 2005;15:1446–1455.
McAllister HA Jr. Primary tumors and cysts of the heart and pericardium. *Curr Probl Cardiol* 1979;4(2):1–51.
McCarthy PM, Piehler JM, Schaff HV, et al. The significance of multiple, recurrent, and complex cardiac myxomas. *J Thorac Cardiovasc Surg* 1986; 91(3):389–396.
Menon SC, Miller DV, Cabalka AK, Hagler DJ. Hamartomas of mature cardiac myocytes. *Eur J Echocardiogr* 2008;9:835–839.
Mirowitz SA, Gutierrez FR. Fibromuscular elements of the right atrium: pseudomass at MR imaging. *Radiology* 1992;182:231–233
Motwani M, Kidambi A, Herzog BA, Uddin A, Greenwood JP, Plein S. MR imaging of cardiac tumors and masses: a review of methods and clinical applications. *Radiology* 2013;268:26–43.
O'Donnell DH, Abbara S, Chaithiraphan V, et al. Cardiac tumors: optimal cardiac MR sequences and spectrum of imaging appearances. *AJR Am J Roentgenol* 2009;193:377–387.
Parmley LF, Salley RK, Williams JP, Head GB 3rd. The clinical spectrum of cardiac fibroma with diagnostic and surgical considerations: noninvasive imaging enhances management. *Ann Thorac Surg* 1988;45:455–465.
Paydarfar D, Krieger D, Dib N, et al. In vivo magnetic resonance imaging and surgical histopathology of intracardiac masses: distinct features of subacute thrombi. *Cardiology* 2001;95(1):40–47.
Pazos-López P, Pozo E, Siqueira ME, et al. Value of CMR for the differential diagnosis of cardiac masses. *JACC Cardiovasc Imaging* 2014;7:896–905.
Prakash P, Kalra MK, Stone JR, Shepard JA, Digumarthy SR. Imaging findings of pericardial metastasis on chest computed tomography. *J Comput Assist Tomogr* 2010;34:554–558.
Rajiah P, Kanne JP, Kalahasti V, Schoenhagen P. Computed tomography of cardiac and pericardiac masses. *J Cardiovasc Comput Tomogr* 2011;5:16–29.
Reynen K. Cardiac myxomas. *N Engl J Med* 1995;333:1610–1617.
Salanitri JC, Pereles FS. Cardiac lipoma and lipomatous hypertrophy of the interatrial septum: cardiac magnetic resonance imaging findings. *J Comput Assist Tomogr* 2004;28:852–856.
Scheffel H, Baumueller S, Stolzmann P, et al. Atrial myxomas and thrombi: comparison of imaging features on CT. *AJR Am J Roentgenol* 2009;192: 639–645.
Seguin JR, Coulon P, Huret C, Grolleau-Roux R, Chaptal PA. Intrapericardial teratoma in infancy: a rare disease. *J Cardiovasc Surg* 1986;27:509–511.
Semionov A, Sayegh K. Multimodality imaging of a cardiac paraganglioma. *Radiol Case Rep* 2016;11:277–281.
Shanmugam G. Primary cardiac sarcoma. *Eur J Cardiothorac Surg* 2006;29: 925–932.
Sparrow PJ, Kurian JB, Jones TR, Sivananthan MU. MR imaging of cardiac tumors. *Radiographics* 2005;25(5):1255–1276.
Sun JP, Asher CR, Yang XS, et al. Clinical and echocardiographic characteristics of papillary fibroelastomas: a retrospective and prospective study in 162 patients. *Circulation* 2001;103(22):2687–2693.
Sütsch G, Jenni R, von Segesser L, Schneider J. Heart tumors: incidence, distribution, diagnosis. Exemplified by 20,305 echocardiographies. *Schweiz Med Wochenschr* 1991;121(17):621–629.
Syed IS, Feng D, Harris SR, et al. MR imaging of cardiac masses. *Magn Reson Imaging Clin N Am* 2008;16:137–164.
Tada H, Asazuma K, Ohya E, et al. Images in cardiovascular medicine. Primary cardiac B-cell lymphoma. *Circulation* 1998;97(2):220–221.
Tomasian A, Iv M, Lai C, Jalili M, Krishnam MS. Cardiac hemangioma: features of cardiovascular magnetic resonance. *J Cardiovasc Magn Reson* 2007;9: 873–876.
Werdan K, Dietz S, Löffler B, et al. Mechanisms of infective endocarditis: pathogen-host interaction and risk states. *Nat Rev Cardiol* 2014;11(1): 35–50.
Zakaria RH, Barsoum NR, El-Basmy AA, El-Kaffas SH. Imaging of pericardial lymphangioma. *Ann Pediatr Cardiol* 2011;4:65–67.